Warm Inflationary Dynamics of Chaplygin Gas Models with Constant Sound Speed

By

Azmat Rustam

CIIT/FA17-RMT-050/LHR

MS Thesis

In

Mathematics

COMSATS University Islamabad

Lahore Campus

Spring, 2019

COMSATS University Islamabad

Warm Inflationary Dynamics of Chaplygin Gas Models with Constant Sound Speed

A Thesis Presented to

COMSATS University Islamabad, Lahore Campus.

In partial fulfillment

of the requirement for the degree of

MS (Master of Science in Mathematics)

By

Azmat Rustam

CIIT/FA17-RMT-050/LHR

Spring, 2019

Warm Inflationary Dynamics of Chaplygin Gas Models with Constant Sound Speed

A Post Graduate Thesis submitted to the Department of Mathematics as partial fulfillment of the requirement for the award of Degree of M.S (Master of Science in Mathematics).

Name	Registration Number
Azmat Rustam	CIIT/FA17-RMT-050/LHR

Supervisor

Dr. Abdul Jawad

Assistant Professor, Department of Mathematics

COMSATS University Islamabad, Lahore Campus

June, 2019

Final Approval

This thesis titled

Warm Inflationary Dynamics of Chaplygin Gas Models with Constant Sound Speed

By

AZMAT RUSTAM

CIIT/FA17-RMT-050/LHR

Has been approved

For the COMSATS University Islamabad (CUI), Lahore Campus.

External Examiner:____________________________________

Dr. Rizwana Kausar

CAMS, UCP Business School, University of Central Punjab, Lahore

Supervisor:____________________________________

Dr. Abdul Jawad

Department of Mathematics, (CUI) Lahore Campus

HoD:____________________________________

Dr. Sarfraz Ahmad

Department of Mathematics, (CUI) Lahore Campus

Declaration

I, **Azmat Rustam** with registration number **CIIT/FA17-RMT-050/LHR** hereby declare that I have produced the work presented in this thesis, during the scheduled period of study. I also declare that I have not taken any material from any source except referred to wherever due, that amount of plagiarism is within acceptable range. If a violation of HEC rules on research has occurred in this thesis, I shall be liable to punishable action under the plagiarism rules of the HEC.

Date: ______________

Azmat Rustam

CIIT/FA17-RMT-050/LHR

Certificate

It is certified that **Azmat Rustam** with **CIIT/FA17-RMT-050/LHR** has carried out all the work related to this thesis under my supervision at the Department of Mathematics, COMSATS Institute of Information Technology, Lahore campus and the work fulfills the requirement for award of MS degree.

Date: __________________

Supervisor:

Dr. Abdul Jawad
Assistant Professor

Head of Department:

Dr. Sarfraz Ahmad
Associate Professor
Department of Mathematics

DEDICATED TO

My Family

Table of Contents

List of Figures

Acknowledgements

All hail to the Almighty **Allah** the most beneficent and benevolent for bestowing me with enough credibility to complete my research work. My significant appreciation to **Hazrat Muhammad (PBUH)** Who is everlastingly a track of direction and learning for mankind.

I would like to acknowledge my warmest thanks to my respected supervisor **Dr. Abdul Jawad**, whose efforts are higly appreciated. His sincere guidance and expert advice have been invaluable throughout all stages of my work. I would express my gratitude to **Dr. Shamaila Rani** for her valuable suggestions. I also admire the help and guidance of HoD of Mathematics Department, **Dr. Sarfraz Ahmad** and other faculty members.

My acknowledgement would be incomplete without thanking the biggest source of my strength, my family. The blessings of my father **Mr. Rustam Ali** and the love and care of my sisters and brothers for helping me at this stage of my life. I thank them for putting up with me in difficult moments and supporting me to follow my dream of getting this degree.

I have great pleasure in acknowledging my gratitude to my friends **Javeria Zafar**, **Asma Aslam**, **Nida Khalid**, **Iram Saleem**, **Sidra Saleem** especially **Muhammad Waseem** and many others, who deserve thanks for helping me whenever i needed. Their support, encouragement and credible ideas have been great contributors in the completion of my MS thesis.

Lahore **Azmat Rustam**
Spring, 2019

Abstract

In this thesis, we consider a warm inflation universe model in the context of generalized Chaplygin gas and modified Chaplygin gas by taking Dirac-Born-Infeld non-canonical scalar field. We determine the two simple potentials which are quartic potential and chaotic potential by considering the first Friedmann equation. Also, we utilize the Anti-de-Sitter warp factor for the Dirac-Born-Infeld inflation. In each model, we consider the constant sound speed and also determine the number of e-folds, scalar as well as tensor power spectrum, scalar spectral index and tensor-scalar ratio in terms of ϕ under slow-roll approximation. We establish that graphical behavior of $r - N$, $n_s - N$ and $\alpha - N$ for Chaplygin gas models are well matched with the 68% and 95% CL constraints of Planck 2018 TT,TE,EE+lowP+lensing data. The graphical behavior represents that the models are compatible with the Planck data in each case.

Chapter 1
Introduction

The term "evolution" is generally related to biological evolution of living things. But such a process in which the planets, stars, galaxies and the formation of universe and time change are also "evolution". All these matters change over time, though the processes involved in it are very different. The universe constituents are about 75% dark energy (DE), 20% dark matter (DM) and 5% are a small part of photons and neutrons. These measurements agree to the validation of the model of hot big bang. This model states that the universe was extremely hot and dense in the early phase and then the universe eventually expanded and cooled down. The model of big bang is consist on general relativity and on simplifying supposition such as homogeneity and isotropy of space. The trend of DM and DE are two important events, which requires a more basic examination of the law of gravity [1].

The branch of the cosmic physics is very dependent on the maximum scale of the entire universe where the effect of gravity power is important. The universe expands rapidly. This long-term expansion acceleration is due to an exotic component, which has negative pressure and generally known as DE. Many models have already been introduced to be a DE candidate and they are cosmological constant [2] quintessence [3], Chaplygin gas (CG) [4] and holographic DE [5]. Instead of many models, the nature of the dark sector is still unknown, i.e., DE and DM. For explanation of cosmic acceleration DE with negative pressure should be a core candidate. DE can be explained with the help of CG due to its negative pressure. The models of the CG in cosmology has three important properties: they express well ordered transition from a rapid change in the universe, they try to explain a united macroscopic phenomenological which is DE and DM and finally, they represents the easiest distortion of the traditional ΛCDM models.

Different models of CG have been proposed [6] till now because it is very effective to describe the expansion of the universe. Its extended form is referred as generalized CG (GCG). Pure CG and GCG are good fluid which initially stays in pressure without fluid-like pressure and later a cosmological constant. The interesting characteristic of CG belongs to the string theory.

String theory is related to the high dimensional universe. Benaoum has been introduced an exotic fluid, titled Modified CG. MCG as a cosmic model has the necessary features. Rudra [7] considered DE in the form of GCCG and investigated its role in an accelerating universe. It was analyzed that GCCG is DE format which is less restricted as compared to MCG. Herrera et al. [8] studied intermediate inflation considering standard and tachyon scalar field. It was Einstein, who first gained the gravity basic law.

The branch of the cosmic physics is very dependent on the maximum scale of the entire universe where the effect of gravity power is important. Inflation is the defensible model that express early physics of the universe. Our universe has recently started a high-speed expansion phase according to observational data. Apart from solving many defects of hot big scenes inflation give us accurate solution to the explanation of universal large-scale structure (LSS). Guth [9] found it for the first time and called it inflation. The hypothesis of inflation [10]-[12] illustrate a foundation of the standard model of modern cosmology [13]-[16]. As we know that inflation presents most captivating solutions of most of the puzzles of big bang model, which are horizon, flatness, homogeneity and monopoles problems [17]. Inflation is a strong, solution to cosmological puzzles because it explains how to a large class of early state is developed in a unique final state, according to our universe.

According to definition, at very high energy it is period of cosmic expansion which is assumed to occur in the early universe, between big-bang nucleosynthesis (BBN). There are two types of inflation: Standard inflation and warm inflation [18, 19]. Warm inflation not only assign the advantages of the standard inflation as resolving horizon, flatness and monopole issues but it also have variation and upgrades. The most important discrimination is the origin of density flow. Slow roll and reheating are two basic regimes in standard inflation. In standard canonical inflation, we have not appropriate candidates to play the role of inflation.

After origination of the Higgs boson [20] it is notable to examine that it is an inflation candidate. In the standard model of the particle physics, the scalar potential of Higgs boson act asymptotically like the self-interacting quartic potential exceptional gauge field theories [21, 22] whether regrettably, this potential tolerate few analytic issues in standard inflation. Setare and Kamali studied a tachyon warm inflation in the brane world [23]. For instance, in the string theory, Dirac-Born-Infeld (DBI) is born in the context of action.

Such ideas can help in the period of non-canonical inflation that is easily commonly connected to slow- roll regime. A type of inflation which is non-canonical version of ultra-slow roll inflation, for which many methods are not frozen on horizontal crossing, but it is rapidly developed on super horizon scales, we pay attention on the simplest chaotic inflation scenario in the non-canonical generalization [24]. This setup suggests that the inflation might be the successful moving into a wrapped area (throat) developed by a D3-brane radial coordinate in compact space. Brane works as vision and according to its movement in the wrapping area, in which there are two versions of brane inflation Infrared (IR) Model [25, 26] and Ultraviolet (UV) Model [27, 28]. In UV model, inflation runs towards the IR side from the UV side in wrapped space, while in IR model, it runs in opposite direction. The DBI inflation may be considered in category of the $k$inflation models so that it is run by a non-canonical scalar field [29]-[40].

In the DBI inflation, the inverse of the Lorentz factor, $c_s = \frac{1}{\gamma}$ is equal to sound speed, the universe stay cold during inflation, and the further procedure known as reheating should be recommended to the ending of inflation to construct the universal potential. The standard model of cosmology would remain partial and extremely unacceptable, without inflation. The most impressive attainment of inflation is to collaborate with the quantum mechanics, including several efforts, inflation has not been supplanted by its numerous challengers [41]-[61]. For modern cosmology this scenario has moderately become an important part.

The inflationary scenario is also responsible for creating the root of all the LSS in universe. This phase of the inflation demand a condition of the negative pressure that may be easily attained by the scalar field. Including remarkable progress in the model independent analysis from productive field theories [62]-[65], inflation is still generally a model dependent phenomenon. In inflationary cosmology the list of models is thus practically incredible [66]. The most important discrimination is the origin of density flow. All interactivity around the inflaton scalar field and other field degrees of freedom are commonly ignored because the universe undergoes an accelerated expansion. On the other side, some groups of inflaton models expelled by current data in the cold inflation framework can be saved in the warm inflation, which is another implement for victorious inflation. In the warm inflationary framework, which has the necessary characteristics that a reheating juncture is overcome at the end of the accelerated expansion due to the decomposition of the inflaton into radiation and particles throughout the slow-roll phase [67, 68].

This thesis is categorize as follows: In chapter **2**, we introduce the theory of inflation and CG models, some basic definitions related to this topic and the equations that governs the inflationary dynamics. In chapter **3**, we consider the quartic potential and chaotic potential in the context of DBI inflation using different CG models. In the last chapter, we finalize the results and discussion.

Chapter 2
Preliminaries

This chapter has the basic concepts for understanding the thesis work. The basic definitions are very useful for the calculations.

2.1 Background of Cosmological Inflation

In physical cosmology, inflation is a theory of exponential expansion of space in the scenario of early universe. The epoch of inflation lasted from 10^{36} seconds after the supposition of the big bang singularity between 10^{33} and 10^{32} seconds after the singularity. The idea of Inflation was first gained in 1979 by theoretical physicist Alan Guth [9] at Cornell university. It was expanded further in the early 1980s. Inflation is called inflaton that thought of being responsible for inflation in the field.

In 1924 Hubble [69] said that redshift of galaxies was proportional to their distance, this information gave the basis for the big bang model of enlarge universe which is the most important model for the universe and its development to the present time. This model was considered to express rapid expansion with the negative pressure of universe. Research shows that universe undergo three main stages after infrastructure, it is the basis of matter, radiation and DE dominance. In 2012, Alan Guth [9] and Andrei Linde [10] got the prize in Fundamental physics due to their creation and evolution of inflationary cosmology. Inflation is considered as a new addition to the big bang model, so it is important to discuss some features of the universe and big bang models before discussing inflation.

2.1.1 Evolution of the universe

Expansion of the universe relay on general relativity and fluid dynamics which are the laws of particle physics. According to the present scientific understanding, collected matters in the clouds which began to condense and rotate, making pyramids of galaxies. In early phase, universe was very hot and dense, so many small elements are produced from protons and neutrons by taking the process of nucleosynthesis at $T \sim 160MeV$. For nuclear fusion required temperature is $T \sim 0.1MeV$, combine protons and neutrons produce heavy elements (H,He,Li).

The stage which come after the nucleosynthesis is known radiation dominated, in this period universe change to an opaque of matter and radiation becomes equal to temperature $T \sim 1MeV$. Energy density of matter dominate when matter and radiation become equal to each other. The temperature of the plasma cools down during the matter epoch because at $T \simeq 3000K$ the evolution of the universe and recombination of electrons take place. In 1915, Einstein represent the universe with a model which consist on mathematics. After the Einstein model, Friedmann gives some important models.

2.2 Scale Factor

The spatial size of universe at given time is known as the scale factor and it is given by $a(t)$. According to modern cosmological observations, it can be defined as "universe is expanding" so, $a(t) > 0$.

2.3 Hubble Parameter

The Hubble parameter is related to "rate of expansion" of the universe. Its mathematically expression is given as

$$H = \frac{\dot{a}}{a}. \tag{2.3.1}$$

The Hubble constant (H_0) denotes the Hubble parameter at current period. To find the value of H_0 many research have done, which is express as

$$H_0 = 10^5\ h\ \ m/s/Mpc \quad \text{and} \quad 1Mpc \cong 3\times 10^{24} cm, \quad h = 0.71^{+0.04}_{-0.03}.$$

2.4 General Relativity

General relativity laws with metric of Friedmann-Robertson-Walker (FRW) gives basis of the modification of universe [70]-[73]

$$ds^2 = -dt^2 + a^2\bigg(\frac{dr^2}{1-kr^2} + r^2(d\theta^2 + \sin^2\theta\phi^2)\bigg), \tag{2.4.1}$$

where a is scale factor and k represent the curvature of universe, if we put $k = 0$ universe represents the spatially flat, for $k = 1$ universe is open (positive curve), for $k = -1$ universe becomes closed (negative curve). Matter which is contained in universe and spatial curvature are associated with the Einstein field equation given as

$$R_{\mu\nu} - \frac{1}{2}Rg_{\mu\nu} + \Lambda g_{\mu\nu} = 8\pi G T_{\mu\nu}, \tag{2.4.2}$$

where $R_{\mu\nu}$ and R are Ricci tensor and Ricci scalar obtained from FRW metric. Λ is cosmological constant which makes the three four of the total energy density. $T_{\mu\nu}$ represents the stress energy density.

$$T_{\mu\nu} = (P + \rho)U^{\mu}V^{\nu} + Pg^{\mu\nu}. \tag{2.4.3}$$

Here, $g^{\mu\nu}$ denotes the metric tensor. Using $T_{\mu\nu} = 0$ (conservation law), we can find the equation of continuity given as

$$\dot{\rho} + 3H(\rho + P) = 0, \tag{2.4.4}$$

Einstein field equation can derive the Friedmann equation due to the stress energy-momentum tensor,

$$H^2 = \frac{1}{3}\Lambda + \frac{8\pi G\rho}{3} - \frac{k}{a^2}, \quad \frac{\ddot{a}}{a} = -\frac{8\pi G}{3}(\rho + 3P) + \frac{\Lambda}{3}. \tag{2.4.5}$$

2.5 Dark Energy and Dark Matter

In physical cosmology, DE is an unknown force that repel things instead of attraction, which generated the accelerated expansion of universe. DE is the major issue of present era. The density of DE is very low ($\sim 7 \times 10^{-30} g/cm^3$) which is less than DM. Astronomers are doing try hard to find out the properties and nature of DE. Recently, we realized that DE have negative pressure. Recent observation shows that our universe 68.3% comprises of DE, 26.8% contain baryonic and non-barynoic dark matter (DM) and 4.9% consist on visible matter [74]. A lot of research had been done by cosmologists to make an agreement, to find the components and their quantities of DM in the our universe.

2.6 Puzzles of Big Bang theory

The big bang model describes the history and evolution of universe, it also explain the many aspects of the observation but there is some theoretical problems which cannot be resolved such as homogeneity, flatness problem, horizon problem and magnetic monopole problem. Due to recent observation it is not possible to ignore them.

2.6.1 Homogeneity

When we observe the universe from our earth and make observation on another planet which is far away from our earth it will look same, this phenomena is called Homogeneity. In all directions universe looks identical due to isotropy. According to CMB observations, many cosmological models which are depend on the supposition that on large scale universe is homogenously and isotropically. But due to the gravity, at small scale it is not difficult to make observation, after the generation of stars, planets, clusters and galaxies.

2.6.2 Horizon Problem

To describe this problem some cosmological distances are defined. First, we discuss the Hubble radius given as

$$R_H = \frac{c}{H}, \tag{2.6.1}$$

where c is constant sound of speed. Hubble radius gives the information about the particles either they are apathetically connected or nor. If the distance between the two particles are greater than Hubble radius, its mean they cannot communicate with each other. By using FRW metric we can determine the distance in a specific era which is traveled by the light. For $ds^2 = 0$, integration of the following equation describe the comoving distance at time t and signal of light is sent at $t = 0$

$$\iota(t) = \int_0^t \frac{cdt'}{at'}. \tag{2.6.2}$$

As we know that universe increasing, this distance is expand due to a factor $a(t)$. This physical distance known as particle horizon, mathematically written as

$$\iota_p(t) = a(t) \int_0^t \frac{cdt'}{at'}. \tag{2.6.3}$$

If particle horizon has less distance than the distance between two particles, then they never interface. Therefore, there might be another option so that these particles are not contact now as they are disparate due to a distance which has larger value than R_H but they can communicate first, as the distance is smaller than particle horizon which separates them. CMB observations observe 3000 areas that were never in touch. The horizon problem is, why temperature differences is very small between the regions which were never in touch.

2.6.3 Flatness Problem

The alleged fact of observation reveals that flatness puzzle is that there is flat spatial geometry in the universe. Considering the models of FRW which are the models of GTR, cosmic principle choose a set of high symmetric spacetime. These models have three different types of curvature k at $k = 1$ it behaves like sphere, at $k = -1$ it looks like hyperboloid and at $k = 0$ it is a plan. We consider the FRW equation

$$H^2 = \frac{1}{3}\rho - \frac{k}{a^2}, \tag{2.6.4}$$

written as

$$1 - \Omega = \frac{-k}{(aH)^2}, \tag{2.6.5}$$

A density parameter has following form

$$\Omega = \frac{\rho}{\rho_c}.$$

ρ_c is critical density defined as $\rho_c = \frac{3H^2}{8\pi G}$. If average density comes close to critical density the universe becomes flat i.e. $\Omega = 1$. According to recent observation's result the universe looks almost flat. The FRW equation give the information that derivation from flatness related to the expansion of universe. Today, a very small derivation is required to notice the flat universe after the big bang, the value of Ω must be $\Omega = 1 \pm 1 \times 10^{-60}$ at given time, which looks impossible.

2.6.4 Magnetic Monopole problem

As we know that magnetic refer to a magnet and monopole means one pole so, a magnet with one pole called magnetic monopole. Superstring and Grand Unified Theories (GUT) specify the existence there. GUT and hot big bang theories combined each other and give the hypothesis about the large number of monopole but still, there is not a magnetic monopole has been detected.

2.7 Inflation as a Solution

The hypothesis of inflation illustrate a foundation of the standard model of modern cosmology. Alan Guth [9] found it for the first time and called it inflation. Inflationary models have ability to give the solution of the problems of big bang theory which we discussed above. Now we can explain briefly how this model give the solution of many problems.

Homogeneity problem

Due to gravitational attraction inhomogeneities produce during inflation. The universe due to its exponential expansion pulls away the gravitationally interacting particles, so the evolution of inhomogeneity is not possible. After the period of inflation the universe become homogeneous. But at the end of inflationary era quantum fluctuation generates small inhomogeneities. These small inhomogeneities causes the large scale structures.

Horizon problem

Horizon problem can be determine as during inflationary era universe increases exponentially. During inflation the expression of particle horizon is

$$\iota_p(t) = \frac{1}{H_0}(e^{H_0 t} - 1). \tag{2.7.1}$$

So, as the time has passed the particle horizon increased. Therefore, during inflation the Hubble radius remain constant and it is given as $R_H = \frac{1}{H_0}$. Thus, particle horizon spread exponentially and become larger than Hubble radius. Those particles which cannot interact now because they are isolated by the distance which is very large as compared to the Hubble radius. Hence, the problem of horizon is solved.

Flatness problem

Inflation also give the solution for the flatness problem. Considering the development of the density parameter which is mentioned in Eq.(3.1.10) it is observed that without fine tuning accelerating scale factor leads the universe towards the flatness.

Magnetic monopole problem

Scale factor during the inflation grows by a extensive factor. However, energy density which may be exist earlier to inflation is weaken to nothing, on the other hand it gives rapid expansion pressing any monopole density. Due to this reason, we will not notice the any magnetic monopole.

2.8 Inflationary Dynamics

Inflationary era is a time period in which our universe undergoes an accelerated expansion due to scale factor which is increased. Inflation occur when

$$\ddot{a} > 0. \tag{2.8.1}$$

Considering the Friedman equation with the continuity equation, condition which is necessary for inflation is

$$\rho + 3P < 0. \tag{2.8.2}$$

Therefore, density of matter is positive which shows that negative pressure is required for the inflation. For the model of inflation it is suppose that universe have inflatons at the inflationary time. The equation of state (EoS) of these inflatons has negative pressure and they are spin 0 particles. These type of particles are found in the theories of particle physics, symmetry of the fundamental forces are due to these particles. During the era of inflation universe become supercools and at the end of inflation reheating is start in which baryogenesis and nucleosynthesis processes take place. After that unverse undergoes radiation, phase transition and then matter dominated era. Also, for the model of inflation scalar field is very important.

Original model of Guth's [9, 17] is also known old inflation, he considered the first order transition of phase, according to it scalar field goes to false vacuum state to true state, but it is not attainable due to potential hurdle between them and at high temperature it undergo in the false vacuum state. When the temperature decreased the true vacuum state become lower and lower, then at some point scalar field shift to the true vacuum state. High entropy produce due to the extreme energy which is released in the form of heat. In this way flatness and horizon problems are solved. Evolution of the bubbles is failing in the original model. So, expansion of the universe is faster than growth of the bubbles. In the other words, inflation never stop, this puzzle is called graceful exist puzzle.

In 1982 a new model of inflation which is called new inflation was suggested by Linde [10], Albrecht and steinhardt [11]. Second ordered of phase transition is considered by Linde, he observed that no bubbles are produced and entire universe enters in the true vacuum state. To avoid it immediately, there is required a flat potential. Therefore, initial conditions must satisfy by the scalar field $(\phi = 0), (\dot{\phi} = 0)$. Linde also give the concept of chaotic inflation, in which universe was initially in chaotic state where scalar field have any value. In the era of Planck this is happened where quantum effects dominate the universe. Before, the era of Planck the effects of quantum are subdominant and scalar field act classically, that means field rolls down the potential and inflation is achieved the success. For scalar field Lagrangian L has the following expression

$$L = -\frac{1}{2}\eta^{\mu\nu}\frac{\partial\phi}{\partial x^{\mu}}\frac{\partial\phi}{\partial x^{\nu}} - V(\phi). \tag{2.8.3}$$

Here $V(\phi)$ is scalar field potential and other term known as kinetic term. Note that dimension of V is $[energy]^4$ and dimension of ϕ is $[energy]^1$. The stress energy momentum tensor and the Lagrangian create the equation for the energy density ρ_ϕ and pressure P_ϕ of the field [75]

$$\rho_\phi = \frac{1}{2}\dot{\phi}^2 + V(\phi) \tag{2.8.4}$$

$$P_\phi = \frac{1}{2}\dot{\phi}^2 - V(\phi) \tag{2.8.5}$$

If we use above equations in Friedmann equations and set the value $k = 0$ then we can get the following relation

$$\left(\frac{\dot{a}}{a}\right)^2 = \frac{8\pi G}{3}\left(\frac{1}{2}\dot{\phi}^2 + V(\phi)\right) \tag{2.8.6}$$

and equation of continuity give the following expression

$$\ddot{\phi} + 3H\dot{\phi} + V' = 0 \tag{2.8.7}$$

Here, dot shows the derivative w.r.t time and V' means the derivative w.r.t the field. The equation of motion (3.1.18) and harmonic oscillator are equal. These equation can be solved if we calculate the duration of inflationary era which is computed in the form of N and given as

$$N = \ln \frac{a_{t_{end}}}{a_t}. \tag{2.8.8}$$

$a_{t_{end}}$ is a scale factor when inflation is end and a_t known scale factor at the time t. For perturbation of scalar field, we consider the Fourier transform in which each scale is related to wave number denoted by k. The perturbation of scalar field are generated between the Hubble radius in which the period of inflation take place and grow as long as they leave the horizon ($k = aH$). Therefore, $R \equiv \psi + H\frac{\delta\phi}{\phi} \simeq (\frac{H}{\dot{\phi}})(\frac{H}{2\pi})$, here δ_ϕ is consider perturbation of the scalar field ϕ. Power spectrum of curvature perturbation can be obtained as

$$P_R \approx \left(\frac{H^2}{2(\pi)\dot{\phi}}\right)^2. \tag{2.8.9}$$

However, the power spectrum rely on the fluctuation scale k and estimate by the scalar spectral index defined as

$$\eta_s = 1 + \frac{d \ln P_R(k)}{dlnk}. \tag{2.8.10}$$

If the value of η_s is close to 1 its mean a scale invariant spectrum [76, 77].

2.9 Inflationary Dynamics of Slow Roll Era

It is impossible to estimate the analytically correct solutions of the equations of inflation, this encourages the proposition of the standard slow-roll approximation. Due to the slow-roll approximation the equation of inflationary field can be reduced, considering that flat potential $V(\phi)$ rolls down by inflation field, therefore the kinetic energy of inflation $(\frac{\dot{\phi}^2}{2})$ can be negligible. By taking these equations in Friedmann and continuity relations, we can obtain the equation of motion as following

$$H^2 - \frac{1}{3}(\frac{\dot{\phi}^2}{2} + V(\phi)) = 0, \quad \ddot{\phi} + \frac{dV}{d\phi} - 3H\dot{\phi} = 0,$$

Second equation is also known the scalar wave equation. The condition for the inflation must satisfy by the effective energy density and pressure, i.e., $\dot{\phi}^2 \ll V(\phi)$. Due to this approximation second $(\frac{\dot{\phi}^2}{2})$ and first $\ddot{\phi}$ terms of the above equation can be neglected and written as

$$H^2 \simeq \frac{V(\phi)}{3}, \quad 3H\dot{\phi} \simeq -\frac{dV}{d\phi}. \tag{2.9.1}$$

we can give the expressions for Inflationary condition as follow

$$\frac{\ddot{a}}{a} = \dot{H} + H^2 > 0,$$

Above condition will hold only if $\dot{H} > 0$ otherwise $\frac{-\dot{H}}{H^2} < 1$. The standard slow-roll parameters ϵ, η and κ are introduced to determine accuracy of the slow-roll approximation, they are give as

$$\epsilon \equiv \frac{-\dot{H}}{H^2}, \quad \eta \equiv \frac{\ddot{H}}{H\dot{H}} \quad \kappa \equiv \frac{\dot{c}_s}{Hc_s}, \tag{2.9.2}$$

ϵ, η and κ must satisfy the conditions which are $\epsilon \ll 1$, $\eta \ll 1$ and $\kappa \ll 1$. Two Slow-roll parameters ϵ and η known as the first and second Hubble slow-roll parameters and κ is the sound slow-roll parameter respectively.

2.10 Process of Reheating

As we know that temperature of the universe decrease exponentially by the factor $\ddot{a} > 0$, at the end of inflationary era universe comes to supercooled state. So, when inflation ends the big bang process restart for which high temperature is requires in mostly models of inflation a mechanism which is called reheating is introduced for the solution of this problem. During inflation the interaction between inflaton field and other fields can be neglected. Therefore, universe remain cooled during the inflation and additional process known reheating [78]. Alternatively, for the scenario of warm inflation, the interaction of inflation field and other fields play the dynamical roll in the period of inflation [18, 79]. The energy density of inflaton field may be changed to energy density of radiation field, in this way without resorting to any reheating process inflation terminate [80].

2.11 Chaplygin Gas

We discuss a recently suggested class of the models of cosmos which is based on the use of static perfect fluid [81]. Commonly, we work on the simple model of the universe filled with the CG, which is a good fluid given by the equation of state (EoS) as follows

$$P = -\frac{A}{\rho}, \tag{2.11.1}$$

A is the positive constant. And, Chaplygin introduced the above EoS as it is a perfect mathematical approximation so that in aerodynamics we can calculate the lifting force which is on a wing of an airplane. The same was later replaced in the same term [82]. The interesting feature of the CG is related to string theory. String theory is related to high dimensional universe. Monerat et al. [83] discussed the initially universe cosmology and the early condition for inflation and CG. CG has three different model, in our work we consider two models which are Generalized CG (GCG) and Modified CG (MCG). The expanded term of CG known as GCG and its equation of state (EoS) is given as

$$P_{gcg} = -\frac{A}{\rho_{gcg}^{\lambda}}, \tag{2.11.2}$$

where P_{gcg} and ρ_{gcg} represent the pressure and energy density and A is the positive constant and $0 < \lambda \leqslant 1$ respectively . GCG's energy density can be derive using continuity equation which is given as

$$\rho_{gcg} = (A + \frac{B}{a^{3(1+\lambda)}})^{\frac{1}{1+\lambda}}, \tag{2.11.3}$$

where a is the scale factor and B is the positive integration constant. Due to GCG, Friedmann equation written as

$$H^2 = \frac{1}{3M_p^2}\left((A + \rho_{\phi}^{1+\lambda})^{\frac{1}{1+\lambda}} + \rho_R\right). \tag{2.11.4}$$

Due to an extrapolation of Eq.(2.11.6) this modification is feasible so that

$$\rho_{gcg} = (A + \rho_m^{1+\lambda})^{\frac{1}{1+\lambda}} \rightarrow (A + \rho_{\phi}^{1+\lambda})^{\frac{1}{1+\lambda}}, \tag{2.11.5}$$

where ρ_m represent the matter energy density.

For MCG EoS is given as [83]

$$P_{mcg} = \mu\rho_{mcg} - \frac{\nu}{\rho_{mcg}^{\lambda}}, \tag{2.11.6}$$

where P_{mcg} and ρ_{mcg} shows the pressure and energy density and $0 \leq \lambda \leq 1$, μ,ν considered positive constants respectively. We determine the energy conservation equation and show the MCG density, as following

$$\rho_{mcg} = \left(A + \frac{c}{a^{3(1+\lambda)(1+\mu)}}\right)^{1+\lambda}, \tag{2.11.7}$$

where c denote the constant of integration and $A = \frac{\nu}{1+\mu}$. We start with the modified Friedmann equation which has the following form

$$H^2 = \frac{1}{3M_p^2}\left((A + \rho_{\phi}^{(1+\lambda)(1+\mu)})^{1+\lambda} + \rho_R\right) \tag{2.11.8}$$

the above relation is occurred because of an extrapolation of Eq.(2.11.7) so that

$$\rho_{mcg} = \left(A + \rho_m^{(1+\lambda)(1+\mu)}\right)^{1+\lambda} \rightarrow \left(A + \rho_{\phi}^{(1+\lambda)(1+\mu)}\right)^{1+\lambda} \tag{2.11.9}$$

where ρ_m represent the matter energy density.

2.12 Chaotic and Quartic Potential

Chaotic inflationary scenario resolved the many problems of old and new inflation. Due to this scenario, in the early universe inflationary era may begin even if there was no thermal equilibrium occur. Chaotic potential is simplest model of the scalar field ϕ having mass m and potential $V = \frac{(m\phi)^2}{2}$ [84]. Quartic potential, which is consider a simplest Higgs potential $V(\phi) = \frac{\lambda\phi^4}{4}$ given by particle physics in the theories of renormalizable, since it gives the information about too many gravity waves. Also, the presence of a non-minimal coupling can make the quartic potential workable [85]. A simple chaotic inflation can be determine by this potential[12].

2.13 DBI Non-canonical Scalar Field

An interesting inflaton candidate encouraged the string theory has been suggested in the context of DBI inflation. However, non-canonical kinetic energy of a single field can drive the inflation. Generally, the non-canonical inflationary model are mention in the class of "k-inflation". In k-inflation models, we can referred the DBI and Tachyonic models.

Chapter 3
Warm DBI Inflation with Quartic and Chaotic Potential using Chaplygin Gas Models

In this chapter, we develop the warm inflation universe model in the context of generalized chaplygin gas and modified chaplygin gas models in the light of Dirac-Born-Infeld (DBI) non-canonical scalar field. We will discuss the two simple potentials which are quartic potential and chaotic potential considering the first Friedmann equation. Also, we utilize the Anti-de-Sitter warp factor for the Dirac-Born-Infeld inflation. In each model we consider the constant sound speed and also utilize the expression for inflationary parameters in terms of ϕ under slow-roll approximation.

3.1 Background Of Warm Inflationary Scenario

In warm inflationary scenario, in the appearance of standard scalar field for the flat FRW universe first Friedmann equation determine as

$$H^2 = \frac{1}{3M_p^2}(\rho_\phi + \rho_R). \tag{3.1.1}$$

where ρ_R and ρ_ϕ are the radiation and energy density of inflaton. The inflaton scalar field connect with the other fields in the warm inflation and dissipation plays a dynamic behavior during inflation. Due to dissipative results, the vacuum energy converted in the form of radiation energy. In the presence of energy density and radiation, we have the following conservation equations

$$\dot{\rho_\phi} + 3H(\rho_\phi + p_\phi) = -\Upsilon(\rho_\phi + p_\phi), \quad \dot{\rho_R} + 3H(\rho_R + p_R) = \Upsilon(\rho_\phi + p_\phi) \tag{3.1.2}$$

Here Υ is the dissipation parameter which depends upon inflaton field as well as temperature and it can be resolute in quantum field theory [86]. It is noticed that radiation energy satisfy the black body equation $\rho_R = \alpha T^4$ in warm inflation. Here, $\alpha = \frac{\pi^2 g_*}{30}$, present the Stefan-Boltzmann constant while $g_* = 228.75$ is the relativistic level of freedom [87] also T is the temperature of thermalize bath.

Therefore, energy density as well as pressure regarding DBI scalar field are denoted by

$$\rho_\phi \equiv 2X\mathcal{L}_{,X} - \mathcal{L} = \frac{\gamma - 1}{f(\phi)} + V(\phi), \quad p_\phi \equiv \mathcal{L} = \frac{\gamma - 1}{\gamma f(\phi)} - V(\phi), \quad (3.1.3)$$

where $V(\phi)$ and $f(\phi)$ are the potential energy and the warp factor of the inflaton, respectively. Also, $\mathcal{L}_{,X} \equiv \frac{\partial \mathcal{L}}{\partial X}$ and γ is the Lorentz factor defined as

$$\gamma \equiv \frac{1}{\sqrt{1 - f(\phi)\dot{\phi}^2}}. \quad (3.1.4)$$

The slow-roll parameters take the following forms [88]-[90]

$$\epsilon \equiv -\frac{\dot{H}}{H^2}, \quad \eta \equiv \frac{\dot{\epsilon}}{H\epsilon}, \quad \kappa \equiv \frac{\dot{c}_s}{Hc_s}. \quad (3.1.5)$$

Moreover, the speed of sound in the scenario of DBI scalar field can be given as

$$c_s^2 \equiv \frac{\partial p_\phi / \partial X}{\partial \rho_\phi / \partial X} = \frac{1}{\gamma^2} = 1 - f(\phi)\dot{\phi}^2. \quad (3.1.6)$$

It illustrated that speed of propagation of density perturbations should be real and subluminal, $0 < c_s^2 \leqslant 1$. In the onward work, we consider the squared speed to be constant. In view of squared speed of sound, Eqs.(3.1.3) can be re-written as

$$\rho_\phi = \frac{\dot{\phi}^2}{c_s(1 + c_s)} + V(\phi), \quad p_\phi = \frac{\dot{\phi}^2}{1 + c_s} - V(\phi). \quad (3.1.7)$$

By substituting the derivative of Eq.(3.1.2) in Eq.(3.1.7), one can get

$$\frac{2\ddot{\phi}}{1+c_s} + (3H+\Upsilon)\dot{\phi} + c_s V\acute{(}\phi) \;\; = \;\; 0. \tag{3.1.8}$$

Also, throughout the warm inflationary scenario the quasi-stable production of photons is, i.e. $\dot{\rho}_R \ll 4H \ \rho_R$. Moreover, we realized that the energy density of inflation control the density of radiation energy at the initial stage of inflation , i.e. $\rho_\phi \gg \rho_R$. In view of these ideas, one can obtain the following expressions from Eqs.(3.1.2) and (3.1.8) as

$$(3H+\Upsilon)\dot{\phi} + c_s V'(\phi) \approx 0, \tag{3.1.9}$$

$$\rho_R \approx \frac{3Q\dot{\phi}^2}{4c_s}. \tag{3.1.10}$$

It is easy to implement the Hamilton-Jacobi formalism [91]-[93], where the Hubble parameter H is consider the function of inflation field ϕ. This form was firstly developed [27] in the setting of DBI inflation and it was investigated in [94]. According to this formalism the slow roll parameters reduce to the following form [88]-[90]

$$\tilde{\epsilon} \;\; \equiv \;\; \frac{2M_p^2}{\gamma}\left(\frac{H'}{H}\right)^2, \tag{3.1.11}$$

$$\tilde{\eta} \;\; \equiv \;\; \frac{2M_p^2}{\gamma}\frac{H''}{H}, \tag{3.1.12}$$

$$\tilde{\kappa} \;\; \equiv \;\; \frac{2M_p^2}{\gamma}\frac{H'}{H}\frac{\gamma'}{\gamma}. \tag{3.1.13}$$

Note that the stability of the above analysis rely on the behavior of a new slow-roll parameter [95]

$$\tilde{\sigma} \equiv 2M_p^2 c_s \frac{\Upsilon'}{\Upsilon}\frac{H'}{H}. \tag{3.1.14}$$

During the inflation, size of the universe is usually represented by number of e-fold

$$N \equiv \ln\left(\frac{a_e}{a}\right), \tag{3.1.15}$$

where a_e at the end of inflation is the scale factor of the universe. It is sure that in the observable universe, the largest scale at $N_* \approx 50 - 60$ e-folds left the horizon from the end of inflation [96, 97]. We use the following expression for the number of e-folding

$$\begin{aligned} dN &= -Hdt \\ d\ln\kappa \approx Hdt &= -dN. \end{aligned} \tag{3.1.16}$$

The scalar spectral index is define to measure the scale-dependence of the scalar power spectrum as

$$n_s - 1 \equiv \frac{d\ln P_s}{d\ln\kappa}. \tag{3.1.17}$$

In DBI model, the tensor power spectrum is written as [98, 99]

$$P_t = \frac{2H^2}{\pi^2 M_p^2}. \tag{3.1.18}$$

In the tensor-to-scalar ratio, an important inflationary observable is defined as

$$r \equiv \frac{P_t}{P_s}. \tag{3.1.19}$$

This amount has a special importance in distinguish around non-identical inflationary models. In fact, in the light of the calculated data, combining of the observational bounds of r and n_s provide a powerful criterion to discriminate between the usable inflationary models. In the DBI warm inflation, beyond the sound horizon scales, the curvature perturbations can be calculated and the power spectrum of the curvature perturbations can be gained after complement to the perturbations eliminate at the smaller thermal noise scales,

$$P_s = \frac{\sqrt{3}}{16\pi^{\frac{3}{2}} M_p^2} \frac{HT}{c_s \tilde{\epsilon}} (1+Q)^{\frac{5}{2}}. \tag{3.1.20}$$

Also, the tensor perturbation are disconnect from the thermal perturbations. Moreover, in cold and warm inflation the tensor power spectra is same. Therefore, tensor-to-scalar ratio $r = \frac{P_t}{P_s}$ becomes smaller in the warm inflation than in cold. where

$$Q \equiv \frac{\Upsilon}{3H} \quad \text{where} \quad \Upsilon = 3HQ. \tag{3.1.21}$$

Also, running of the scalar spectral index can be defined as

$$\alpha = \frac{dn_s}{dln\kappa} \quad = \quad -\frac{d}{dN}(n_s). \tag{3.1.22}$$

We assume the following AdS warp factor in our work [27, 100, 101]

$$f(\phi) = \frac{f_0}{\phi^4}, \tag{3.1.23}$$

where f_0 represents a positive dimensionless constant. Due to above relation Eq.(3.1.23), Eq.(3.1.6) leads to

$$\dot{\phi} = -\sqrt{\frac{1-c_s^2}{f_0}}\phi^2. \tag{3.1.24}$$

Putting this into Eqs. (3.1.9) and (3.1.10), respectively, we obtain

$$Q \;=\; \frac{-c_s V'(\phi)}{3H\dot{\phi}} - 1, \tag{3.1.25}$$

$$T \;=\; \left(\frac{3Q(1-c_s^2)\phi^4}{4c_s\alpha f_0}\right)^{\frac{1}{4}}. \tag{3.1.26}$$

If we solve the differential Eq.(3.1.24), inflationary field evolution can be determine as

$$\phi = \sqrt{\frac{f_0}{1-c_s^2}\frac{1}{t}}, \tag{3.1.27}$$

where we take the integration constant to be zero.

3.2 Chaplygin Gas Models With Chaotic Potential

We consider the CG models using the chaotic potential $V(\phi) = \frac{(m\phi)^2}{2}$, here ϕ represents the scalar field and m denote the mass of scalar field. It is a simplest model of a scalar field. Various generalization of CG has been suggested as it is very effective for exploring the cosmic expansion. In our work we use two models of CG which are

- GCG
- MCG

3.2.1 Generalized Chaplygin Gas

It is noticed that CG is an alternate description of accelerating expansion. In $(d+1, 1)$ space time CG appears as a powerful fluid of generalized D-brane and the action can be given in the form of generalized born-infield [104]. Kammshchick [4] noticed that FRW universe consisted of the CG which express that universe is in the good agreement with the recent observation of cosmic acceleration. In the duration of inflationary period, energy density of the scalar field dominated by the energy density of radiation field as we mention above, i.e., $\rho_\phi \gg \rho_R$ and $\rho_\phi \sim V$. Here, $\lambda = 1$ so that, the Friedmann equation becomes

$$H^2 = \frac{1}{3M_p^2}\sqrt{A + \rho_\phi^2} \sim \frac{1}{3M_p^2}\sqrt{A + V^2} \tag{3.2.1}$$

Now, we construct the inflationary parameters for the case of GCG. Considering Eqs.(3.1.11), (3.1.25), (3.1.26), (3.2.1) and chaotic potential in terms of ϕ and inserting the results in Eq. (3.1.20) we get the power spectrum of curvature perturbation as

$$
\begin{aligned}
P_s &= \gamma\Bigg((c_s m^2 M_p)\times(\sqrt{\frac{1-c_s^2}{f_0}}\phi(4A+m^4\phi^4)^{\frac{1}{4}})^{-1}\Bigg)^{\frac{5}{2}}(4A+m^4\phi^4)^{\frac{9}{4}} \\
&\times \Bigg(\phi^3(\frac{3(-1+c_s^2)\phi}{c_s f_0})+\frac{\sqrt{\frac{6-6c_s^2}{f_0}}m^2M_p}{(4A+m^4\phi^4)^{\frac{1}{4}}}\times(\alpha)^{-1}\Bigg)^{\frac{1}{4}}\Bigg(482^{\frac{3}{4}}3^{\frac{1}{4}}c_s m^8 \\
&\times M_p^5\phi^{\frac{3}{2}}\phi^6\Bigg)^{-1}. \qquad (3.2.2)
\end{aligned}
$$

Similarly we can drive the expression for number of e-fold in term of ϕ by using the Eqs.(3.1.24) and (3.2.1) as

$$
\begin{aligned}
N &= -\Bigg(-12(4A+m^4\phi^4)+\sqrt{2}m^4\phi^4(4+\frac{m^4\phi^4}{A})^{\frac{3}{4}}Hypergeometric2F1 \\
&\times [\frac{3}{4},\frac{3}{4},\frac{7}{4},-\frac{m^4\phi^4}{4A}]\Bigg)\times\Bigg(12\sqrt{\frac{6-6c_s^2}{f_0}}M_p\phi(4A+m^4\phi^4)^{\frac{3}{4}}\Bigg)^{-1}. \quad (3.2.3)
\end{aligned}
$$

We can determine the scalar spectrum index by using Eqs.(3.1.16),(3.1.17) and (3.2.2) as

$$
\begin{aligned}
n_s &= 1-3(-1+c_s^2)M_p\phi\Bigg(-62Ac_s m^2M_p-3c_s m^6M_p\phi^4+\sqrt{\frac{6-6c_s^2}{f_0}} \\
&\times 30A\phi(4A+m^4\phi^4)^{\frac{1}{4}}+\sqrt{\frac{6-6c_s^2}{f_0}}m^4\phi^5(4A+m^4\phi^4)^{\frac{1}{4}}\Bigg)\times\Bigg((4A \\
&+ m^4\phi^4)^{\frac{5}{4}}(c_s\sqrt{\frac{6-6c_s^2}{f_0}}f_0m^2M_p-3\phi(4A+m^4\phi^4)^{\frac{1}{4}}+3c_s^2\phi \\
&\times (4A+m^4\phi^4)^{\frac{1}{4}})\Bigg)^{-1}. \qquad (3.2.4)
\end{aligned}
$$

By using the Eq.(3.1.22) we can get the value of the running of scalar spectral index as

$$
\begin{aligned}
\alpha &= \Bigg(18(-1+c_s^2)M^2\phi^2\Bigg(c_s\sqrt{\frac{6-6c_s^2}{f_0}}f_0m^{10}M_p\phi^9(4A+m^4\phi^4)^{\frac{1}{4}}-2Am^4 \\
&\times \phi^4\Bigg(-99c_s\sqrt{\frac{6-6c_s^2}{f_0}}f_0m^2M_p\phi(4A+m^4\phi^4)^{\frac{1}{4}}+150\phi^2\sqrt{4A+m^4\phi^4}
\end{aligned}
$$

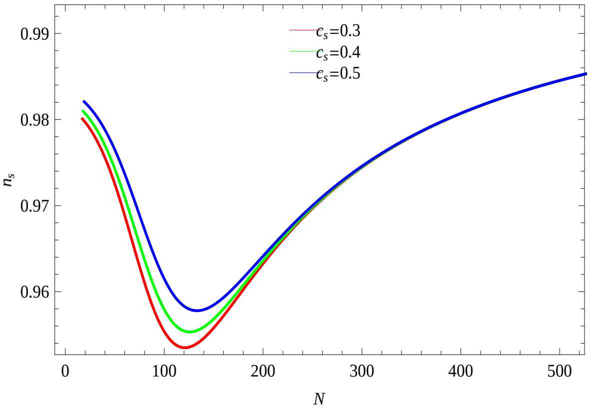

Figure 3.1: Plot of n_s versus N for different values of c_s. The values of other parameters are $M_p = 1$, $\lambda = 1$, $A = 4$, $f_0 = 12095.1$, $\alpha = 0.5$ and $m = 2$. We can find the best range of n_s where $60 < N$.

$$
\begin{aligned}
&+ \quad 2c_s^2(47f_0m^4M^2 - 75\phi^2\sqrt{4A + m^4\phi^4})\Big) + 8A^2\Big(- 30c_s\sqrt{\frac{6 - 6c_s^2}{f_0}}f_0m^2 \\
&\times \quad M_p\phi(4A + m^4\phi^4)^{\frac{1}{4}} + 45\phi^2\sqrt{4A + m^4\phi^4} + c_s^2(31f_0m^4M^2 \\
&- \quad 45\phi^2\sqrt{4A + m^4\phi^4})\Big)\Big)\Big) \times \Big(f_0(4A + m^4\phi^4)^{\frac{5}{4}}(c_s\sqrt{\frac{6 - 6c_s^2}{f_0}} \\
&\times \quad f_0m^2M_p - 3\phi(4A + m^4\phi^4)^{\frac{1}{4}} + 3c_s^2\phi(4A + m^4\phi^4)^{\frac{1}{4}})^2\Big)^{-1}. \qquad (3.2.5)
\end{aligned}
$$

By inserting the Eqs.(3.1.18) and (3.2.2) into Eq.(3.1.19) expression for the tensor-to-scalar ratio turns out . In this way, we can get the following form

$$
\begin{aligned}
r \quad &= \quad \Big(16 \times 2^{\frac{3}{4}}3^{\frac{1}{4}}c_sm^8M_p\phi^6\Big) \times \Big(\gamma\Big((c_sm^2M_p) \times (\sqrt{\frac{1 - c_s^2}{f_0}}\phi(4A \\
&+ \quad m^4\phi^4)^{\frac{1}{4}})^{-1}\Big)^{\frac{5}{2}}(4A + m^4\phi^4)^{\frac{7}{4}}\Big(\phi^3(\frac{3(-1 + c_s^2)\phi}{c_sf_0}) + \frac{\sqrt{\frac{6-6c_s^2}{f_0}}m^2M_p}{(4A + m^4\phi^4)^{\frac{1}{4}}} \\
&\times \quad (\alpha)^{-1}\Big)^{\frac{1}{4}}\Big)^{-1}. \qquad (3.2.6)
\end{aligned}
$$

Figure **3.1** presented the graph of $n_s - N$ in warm DBI inflationary

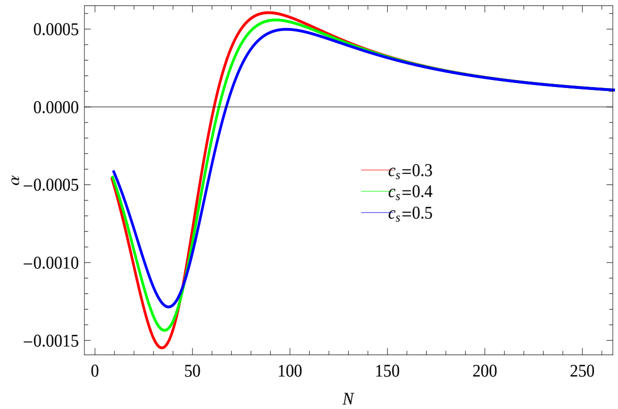

Figure 3.2: Plot of α versus N for different values of c_s. The values of other parameters are $M_p = 1$, $\lambda = 1$, $A = 4$, $f_0 = 3095.1$, $\alpha = 0.5$ and $m = 2$. We can find the best range of α where $60 < N$.

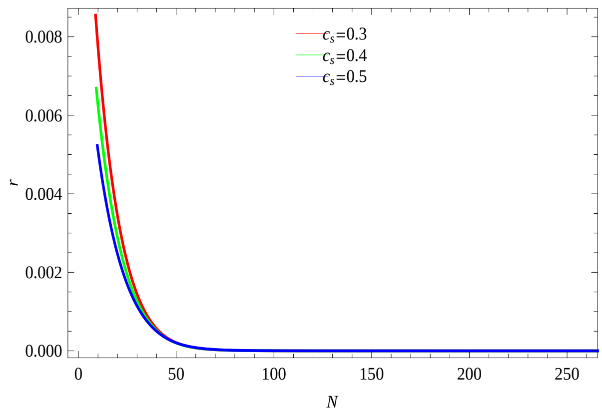

Figure 3.3: Plot of r versus N for different values of c_s. The values of other parameters are $M_p = 1$, $\lambda = 1$, $A = 4$, $f_0 = 3095.1$, $\alpha = 0.5$ and $m = 2$. We can find the best range of r where $60 < N$.

scenario in the presence of chaotic potential. The interval of red trajectory at $c_s = 0.3$ for n_s lies in the interval $[0.95125, 0.98]$ for the desired e-folds number. At $c_s = 0.4$ green trajectory for n_s lies in interval $[0.95375, 0.98125]$. Similarly, at $c_s = 0.5$ blue trajectory for n_s lies in the interval $[0.95875, 0.9825]$ for the desired e-folds number. For $60 < N$ we can see the spectral index is compatible with constraints Planck TT,TE,EE+lowP+lensing data 2018 range which is 0.9649 $\pm$0.0042 [105].

Figure **3.2** shows the behavior of α versus N for chaotic potential. At $c_s = 0.3$ red trajectory for α lies in the interval of $[-0.0016, 0, 0006]$. At $c_s = 0.4$ green trajectory for α lies in the interval of $[-0.00155, 0, 00055]$. At $c_s = 0.5$ blue trajectory for α lies in the interval of $[-0.0013, 0, 0005]$. These interval are well matched with constraints Planck TT,TE,EE+lowP+lensing data 2018 [105]. Figure **3.3** indicates the $r - N$ plane for chaotic potential in the set up of inflationary model. The intervals $[0, 0.00525]$, $[0, 0.00675]$, $[0, 0.0085]$ for red, green and blue lines shows the behavior of our graphs which is comparable with the constraints of Planck TT,TE,EE+lowP+lensing data 2018 [105].

3.2.2 Modified Chaplygin Gas Model

For MCG EoS is given as above [83] so that Friedmann equation adopt the following expression

$$H^2 = \frac{1}{3M_p^2}\left(A + \rho_\phi^{(1+\lambda)(1+\mu)}\right)^{1+\lambda} \sim \frac{1}{3M_p^2}\left(A + V^{(1+\lambda)(1+\mu)}\right)^{1+\lambda} \qquad (3.2.7)$$

Now, we can construct the inflationary parameters for the case of MCG. Considering Eqs.(3.1.11), (3.1.25), (3.1.26), (3.2.7) and chaotic potential in terms of ϕ and inserting the results in Eq. (3.1.20) we get the power spectrum of curvature perturbation as

$$\begin{aligned}
P_s &= 2^{-\frac{7}{2}+2(\lambda+\mu+\lambda\mu)}\gamma m^2\phi(m^2\phi^2)^{-2(1+\lambda)(1+\phi)}(2^{-(1+\lambda)(1+\mu)}(m^2\phi^2)^{(1+\lambda)(1+\mu)} \\
&+ A)^2\left(c_sM_pm^2(\sqrt{\frac{1-c_s^2}{f_0}}\sqrt{(A+2^{-(1+\lambda)(1+\mu)}(m^2\phi^2)^{(1+\lambda)(1+\mu)})^{\frac{1}{1+\lambda}}})^{-1}\right)^{\frac{3}{2}} \\
&\times \left((1-c_s^2)\phi^4\times\left(\frac{c_sM_pm^2}{\sqrt{\frac{3-3c_s^2}{f_0}}\sqrt{(A+2^{-(1+\lambda)(1+\mu)}(m^2\phi^2)^{(1+\lambda)(1+\mu)})^{\frac{1}{1+\lambda}}}}\right.\right. \\
&- \left.\left. 1)\times(c_sf_0\alpha)^{-1}\right)^{\frac{1}{4}}\times\left(3\sqrt{\frac{1-c_s^2}{f_0}}M_p^4\pi^{\frac{3}{2}}(1+\mu)^2\right)^{-1}. \qquad (3.2.8)
\end{aligned}$$

The number of e-folds is given as

$$\begin{aligned}
N &= \sqrt{(A+2^{-(1+\lambda)(1+\mu)}(m^2\phi^2)^{(1+\lambda)(1+\mu)})^{\frac{1}{1+\lambda}}}(1+\frac{2^{-(\lambda)(1+\mu)}(m^2\phi^2)^{(1+\lambda)(1+\mu)}}{A} \\
&+ 1)^{\frac{1}{2(1+\lambda)}}Hypergeometric2F1\times[-\frac{1}{2(1+\lambda)(1+\mu)},-\frac{1}{2(1+\lambda)}, \\
&\times 1-\frac{1}{2(1+\lambda)(1+\mu)},-\frac{2^{-(\lambda)(1+\mu)}(m^2\phi^2)^{(1+\lambda)(1+\mu)}}{A}]\times(\sqrt{\frac{3-3c_s^2}{f_0}} \\
&\times M_p\phi)^{-1}. \qquad (3.2.9)
\end{aligned}$$

We can find the value of scalar spectrum index by using Eqs.(3.1.16),(3.1.17) and (3.2.8) as

$$\begin{aligned}
n_s &= 1-\left(3(1-c_s^2)M_p\phi((m^2\phi^2)^{(1+\lambda)(1+\mu)}\left(2\sqrt{\frac{3-3c_s^2}{f_0}}(2+3\mu)\phi\right.\right. \\
&\times (A+2^{-(1+\lambda)(1+\mu)}(m^2\phi^2)^{(1+\lambda)(1+\mu)})^{\frac{1}{1+\lambda}}-c_sm^2M_p(6+7\mu) \\
&\times \left.\sqrt{(A+2^{-(1+\lambda)(1+\mu)}(m^2\phi^2)^{(1+\lambda)(1+\mu)})^{\frac{1}{1+\lambda}}}\right)+2^{(1+\lambda)(1+\mu)} \\
&\times A\left(2\sqrt{\frac{3-3c_s^2}{f_0}}(7+8\lambda+8(1+\lambda)\mu)\phi\times(A+2^{-(1+\lambda)(1+\mu)}\right. \\
&\times (m^2\phi^2)^{(1+\lambda)(1+\mu)})^{\frac{1}{1+\lambda}}-\sqrt{(A+2^{-(1+\lambda)(1+\mu)}(m^2\phi^2)^{(1+\lambda)(1+\mu)})^{\frac{1}{1+\lambda}}} \\
&\times \left.\left.\left. c_sm^2M_p(15+16\lambda+16(1+\lambda)\mu)\right)\right)\right)\times\left(4(2^{(1+\lambda)(1+\mu)}A(m^2\right. \\
&\times \phi^2)^{(1+\lambda)(1+\mu)})\sqrt{(A+2^{-(1+\lambda)(1+\mu)}(m^2\phi^2)^{(1+\lambda)(1+\mu)})^{\frac{1}{1+\lambda}}}\left(3(1-c_s^2)\right.
\end{aligned}$$

$$
\begin{aligned}
&\times \quad \phi(A+2^{-(1+\lambda)(1+\mu)}(m^2\phi^2)^{(1+\lambda)(1+\mu)})^{\frac{1}{1+\lambda}}+c_s\sqrt{\frac{3-3c_s^2}{f_0}}\\
&\times \quad \sqrt{(A+2^{-(1+\lambda)(1+\mu)}(m^2\phi^2)^{(1+\lambda)(1+\mu)})^{\frac{1}{1+\lambda}}}\\
&\times \quad f_0m^2M_p\Big)\Big). \qquad (3.2.10)
\end{aligned}
$$

Moreover, using the Eq.(3.1.22) the value of running of the scalar spectral index obtain as we calculate in above section.

The value of tensor-to-scalar ratio obtain by plugging the Eqs.(3.1.18) and (3.2.8) into Eq.(3.1.19). In this way, we can obtain the following expression

$$
\begin{aligned}
r \;&=\; 2^{-\frac{9}{2}-2(\lambda+\mu+\lambda\mu)}(m^2\phi^2)^{-2(1+\lambda)(1+\phi)}(2^{-(1+\lambda)(1+\mu)}(m^2\phi^2)^{(1+\lambda)(1+\mu)}\\
&+\; A)^{-2+\frac{1}{1+\lambda}}\sqrt{\frac{1-c_s^2}{f_0}}(1+\mu)^2\Bigg(m^2\sqrt{\pi}\gamma\phi\Bigg(c_sM_pm^2\times(\sqrt{\frac{1-c_s^2}{f_0}}\\
&\times\; \sqrt{(A+2^{-(1+\lambda)(1+\mu)}(m^2\phi^2)^{(1+\lambda)(1+\mu)})^{\frac{1}{1+\lambda}}})^{-1}\Bigg)^{\frac{3}{2}}\Bigg)^{-1}\Bigg(\Bigg(\Big((1-c_s^2)\phi^4\\
&\times\; \Bigg(-1+\frac{c_sM_pm^2}{\sqrt{\frac{3-3c_s^2}{f_0}}\sqrt{(A+2^{-(1+\lambda)(1+\mu)}(m^2\phi^2)^{(1+\lambda)(1+\mu)})^{\frac{1}{1+\lambda}}}}\Bigg)\\
&\times\; (c_sf_0\alpha)^{-1}\Bigg)^{\frac{1}{4}}\Bigg)^{-1}. \qquad (3.2.11)
\end{aligned}
$$

Figure **3.4** show the graph of $n_s - N$ in warm DBI inflationary scenario in the presence of chaotic potential. The intervals $[0.95875, 0.99]$, $[0.95, 0.99125]$, $[0.9525, 0.99125]$ for red, green and blue lines shows the behavior of our graphs which is comparable with constraints of Planck TT,TE,EE+lowP+lensing data 2018 [105]. Figure **3.5** describe the graph of α versus N for chaotic potential. The intervals $[-0.000875, 0.004125]$, $[-0.001, 0.00375]$, $[0.000875, 0.003375]$ for red, green and blue lines shows the behavior of our graphs which is compatible with constraints of Planck TT,TE,EE+lowP+lensing data 2018 [105]. Figure **3.6** indicates the $r - N$

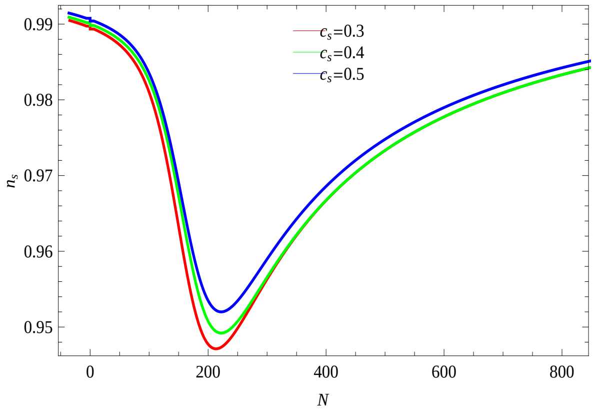

Figure 3.4: Plot of n_s versus N for different values of c_s. We have considered $c_s = 0.3$, $c_s = 0.4$, $c_s = 0.5$, $M_p = 1$, $\lambda = 1$, $A = 4$, $f_0 = 28095.1$, $\alpha = 0.5$, $\mu = 0.7$ and $m = 2$. We can find the best range of n_s where $60 < N$.

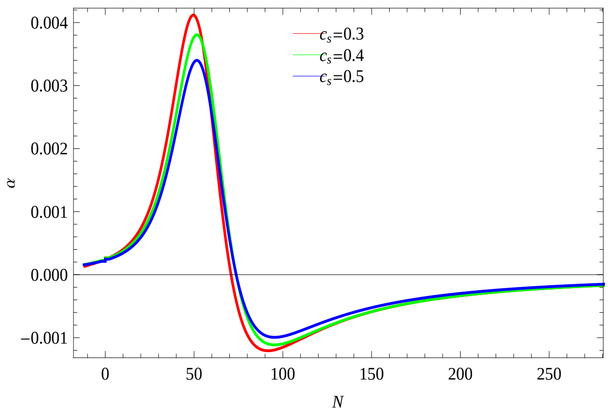

Figure 3.5: Plot of α versus N for different values of c_s. We can find the best range of α where $N > 60$.

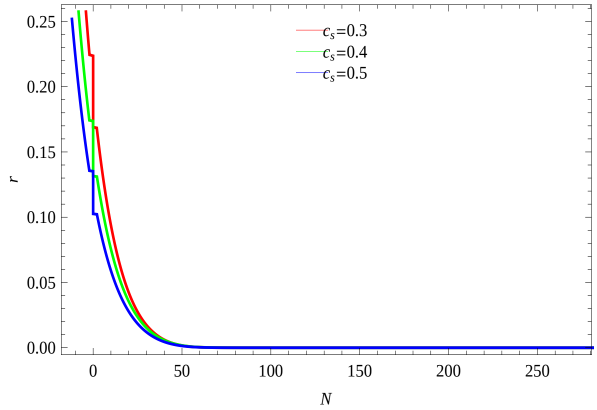

Figure 3.6: Plot of r versus N for different values of c_s. We can find the best range of r where $60 < N$.

plane for chaotic potential in inflationary model. In $r - N$ the intervals $[0, 0.25]$, $[0, 0.25625]$, $[0, 0.25625]$ for red, green and blue lines shows the behavior of our graphs which is well matched with constraints of Planck TT,TE,EE+lowP+lensing data 2018 [105].

3.3 Models of Chaplygin Gas With Quartic Potential

In particle physics theories, we examine a quartic potential $V(\phi) = \frac{\lambda\phi^4}{4}$ which is known as simple Higgs potential [102], where λ is consider a dimensionless parameter. A simple chaotic inflation can be determine by this potential[12] and for the theoretical point of view it has a significant importance, due to its appearance in all renormalizable gauge field theories [102] in which the gauge is impulsively broken along the Higgs mechanism [20]. Quartic potential have some stunning reheating properties [96, 103].

3.3.1 Generalized Chaplygin Gas

With the help of Eqs.(3.1.11), (3.1.25), (3.1.26), (3.2.1) and quartic potential and plugging these results in Eq. (3.1.20) power spectrum can be obtained as

$$\begin{aligned}
P_s &= 8\gamma\Big(A+\frac{\lambda^2\phi^8}{16}\Big)^{\frac{9}{4}}\times\Big(\frac{c_sM_p\lambda\phi}{\sqrt{\frac{1-c_s^2}{f_0}}}(16A+\lambda^2\phi^8)^{\frac{1}{4}}\Big)^{\frac{5}{2}}\times\Big((1-c_s^2)\phi^4\\
&\times\Big(-1+\frac{2c_sM_p\lambda\phi}{\sqrt{\frac{3-3c_s^2}{f_0}}(16A+\lambda^2\phi^8)^{\frac{1}{4}}}\Big)\times(c_sf_0\alpha)^{-1}\Big)^{\frac{1}{4}}\Big(3c_sM_p^5\pi^{\frac{3}{2}}\\
&\times \lambda^4\phi^{14}\Big)^{-1}. \qquad (3.3.1)
\end{aligned}$$

The e-fold number in term of ϕ are calculated by using the Eqs.(3.1.24) and (3.2.1) as

$$\begin{aligned}
N &= -\Big(-28(16A+\lambda^2\phi^8)++\lambda^2\phi^8(16+\frac{+\lambda^2\phi^8}{A})^{\frac{3}{4}}Hypergeometric2F1\\
&\times [\frac{7}{8},\frac{3}{4},\frac{15}{8},-\frac{+\lambda^2\phi^8}{16A}]\Big)\times\Big(56\sqrt{\frac{3-3c_s^2}{f_0}}M_p\phi(16A+\lambda^2\phi^8)^{\frac{3}{4}}\Big)^{-1} \qquad (3.3.2)
\end{aligned}$$

Eqs.(3.1.16),(3.1.17) and (3.3.1) gives the expression for scalar spectral index as follows

$$\begin{aligned}
n_s &= 1-3^{\frac{3}{4}}(1-c_s^2)^2M_p\phi^5(16A+\lambda^2\phi^8)(16A(41c_sM_p\lambda\phi-21\sqrt{\frac{3-3c_s^2}{f_0}}\\
&\times (16A+\lambda^2\phi^8)^{\frac{1}{4}})+\lambda^2\phi^8(-9c_sM_p\lambda\phi+5\sqrt{\frac{3-3c_s^2}{f_0}}(16A+\lambda^2\phi^8)^{\frac{1}{4}}))\Big(\\
&\times 1024c_s(-1+c_s^2)f_0\alpha(A+\frac{\lambda^2\phi^8}{16})^{\frac{5}{2}}\Big(\Big(-1+\frac{2c_sM_p\lambda\phi}{\sqrt{\frac{3-3c_s^2}{f_0}}(16A+\lambda^2\phi^8)^{\frac{1}{4}}}\Big)\\
&\times (1-c_s^2)\phi^4(c_sf_0\alpha)^{-1}\Big)^{\frac{1}{4}}\Big(\Big(\frac{3(-1+c_s^2)}{c_sf_0}+\frac{2\sqrt{\frac{3-3c_s^2}{f_0}}M_p\lambda\phi}{(16A+\lambda^2\phi^8)^{\frac{1}{4}}}\Big)\\
&\times \phi^4(\alpha)^{-1}\Big)^{\frac{3}{4}}\Big)^{-1}. \qquad (3.3.3)
\end{aligned}$$

In addition, the value of running of the scalar spectral index turns out to be

$$
\begin{aligned}
\alpha &= \Bigg(18(-1+c_s^2)^2M_p^2\phi^2\Bigg(3\lambda^4\phi^{16}\Bigg(6c_s\sqrt{\frac{3-3c_s^2}{f_0}}f_0M_p\lambda\phi(16A+\lambda^2\phi^8)^{\frac{1}{4}}\\
&- 5\sqrt{16A+\lambda^2\phi^8}+c_s^2(-6f_0M_p^2\lambda^2\phi^2+5\sqrt{16A+\lambda^2\phi^8})\Bigg)-32A\lambda^2\phi^8\\
&\times \Bigg(458c_s\sqrt{\frac{3-3c_s^2}{f_0}}f_0M_p\lambda\phi(16A+\lambda^2\phi^8)^{\frac{1}{4}}-351\sqrt{16A+\lambda^2\phi^8}+9c_s^2\\
&\times (-50f_0M_p^2\lambda^2\phi^2+39\sqrt{16A+\lambda^2\phi^8})\Bigg)256A^2\Bigg(82c_s\sqrt{\frac{3-3c_s^2}{f_0}}f_0M_p\\
&\times \lambda\phi(16A+\lambda^2\phi^8)^{\frac{1}{4}}-63\sqrt{16A+\lambda^2\phi^8}+9c_s^2(-82f_0M_p^2\lambda^2\phi^2+39\\
&\times \sqrt{16A+\lambda^2\phi^8})\Bigg)\Bigg)\Bigg)\times\Bigg(f_0(16A+\lambda^2\phi^8)\Bigg(48A(-1+c_s^2)+\lambda\phi\\
&\times \Bigg(3(-1+c_s^2)\times\lambda\phi^7+2c_s\sqrt{\frac{3-3c_s^2}{f_0}}f_0M_p(16A+\lambda^2\phi^8)^{\frac{3}{4}}\Bigg)\Bigg)^2\Bigg)^{-1} \qquad (3.3.4)
\end{aligned}
$$

By inserting the Eqs.(3.1.18) and (3.3.1) into Eq.(3.1.19) the expression for tensor-to-scalar ratio takes the following form

$$
\begin{aligned}
r &= \Bigg(c_sM_p^5\lambda^4\phi^{14}\sqrt{64+\phi^8}\Bigg)\times\Bigg(16\gamma\sqrt{\pi}\Bigg(A+\frac{\lambda^2\phi^8}{16}\Bigg)^{\frac{9}{4}}\times\Bigg(\frac{c_sM_p\lambda\phi}{\sqrt{\frac{1-c_s^2}{f_0}}}(16A\\
&+ \lambda^2\phi^8)^{\frac{1}{4}}\Bigg)^{\frac{5}{2}}\times\Bigg((1-c_s^2)\phi^4\times\Bigg(-1+\frac{2c_sM_p\lambda\phi}{\sqrt{\frac{3-3c_s^2}{f_0}}(16A+\lambda^2\phi^8)^{\frac{1}{4}}}\Bigg)\\
&\times (c_sf_0\alpha)^{-1}\Bigg)^{\frac{1}{4}}\Bigg)^{-1}. \qquad (3.3.5)
\end{aligned}
$$

In Figure **3.7** we have plotted the graph of $n_s - N$ in warm DBI inflationary scenario in the presence of quartic potential. The intervals $[0.93025, 1.00125]$, $[0.9305, 1.00125]$, $[0.93125, 1.001]$ for red, green and blue lines shows the behavior of our graphs which is compatible with constraints of Planck TT,TE,EE+lowP+lensing data 2018 [105]. Figure **3.8** describes the behavior of α versus N for quartic potential in the warm DBI inflation.

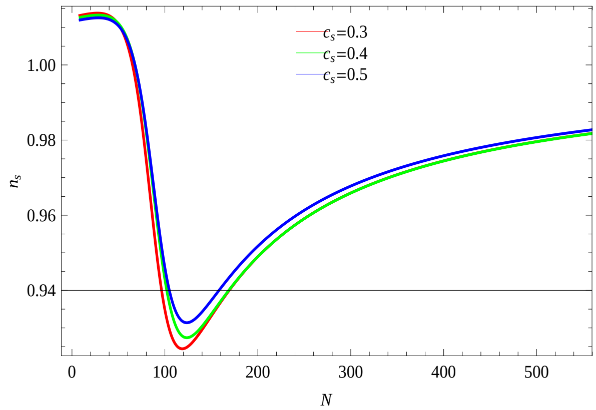

Figure 3.7: Plot of n_s versus N for different values of c_s. We have assumed $c_s = 0.3$, $c_s = 0.4$, $c_s = 0.5$, $M_p = 1$, $\lambda = 1$, $A = 4$, $f_0 = 30095.1$, $\alpha = 0.5$. We can find the best range of n_s where $N > 60$.

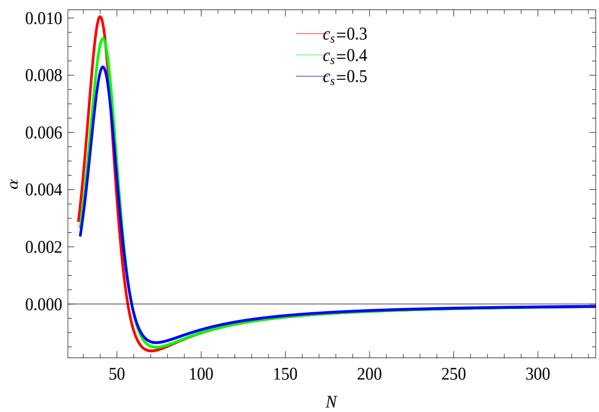

Figure 3.8: Plot of α versus N for different values of c_s. The constants parameters are $c_s = 0.3$, $c_s = 0.4$, $c_s = 0.5$, $M_p = 1$, $\lambda = 1$, $A = 2$, $f_0 = 8095.1$ and $\alpha = 0.5$. We can find the best range of α where $60 < N$.

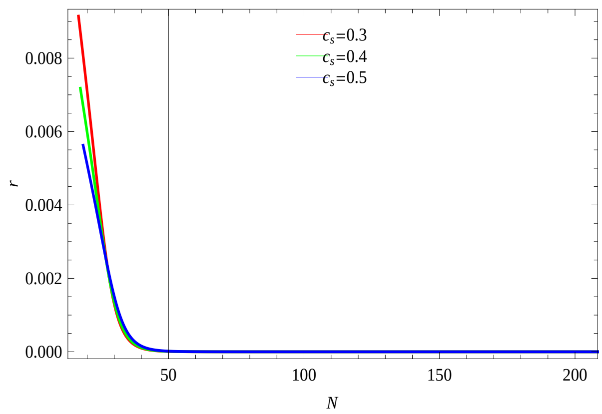

Figure 3.9: Plot of r versus N for different values of c_s. The values of parameters are $c_s = 0.3$, $c_s = 0.4$, $c_s = 0.5$, $M_p = 1$, $\lambda = 1$, $A = 2$, $f_0 = 3095.1$, $\alpha = 0.5$ and $\gamma = \frac{1}{c_s}$. We can find the best range of r where $60 < N$.

The intervals $[-0.0005, 0.010]$, $[-0.0005, 0.00925]$, $[-0.00025, 0.008]$ for red, green and blue lines shows the behavior of our graphs which is compatible with constraints of Planck TT,TE,EE+lowP+lensing data 2018 [105]. Figure **3.9** leads to $r - N$ plane for quartic potential in the current set up of inflationary model. And the intervals $[0, 0.0055]$, $[0, 0.00725]$, $[0, 0.0085]$ for red, green and blue lines represent that our graphs are well matched with observational TT,TE,EE+lowP+lensing data 2018 [105].

3.3.2 Modified Chaplygin Gas Model

We can construct the inflationary parameters for the case of MCG. Expression for P_s, n_s, α and r are given below which is derive as we calculate these expression in the above section.

$$\begin{aligned} P_s &= 2^{-\frac{7}{2}+4(\lambda+\mu+\lambda\mu)}\gamma(\lambda\phi^4)^{-3(\lambda+\mu+\lambda\mu)}(A+4^{-(1+\lambda)(1+\mu)}(\lambda\phi^4)^{(1+\lambda)(1+\mu)})^2 \\ &\times \left(c_s M_p \lambda\phi \times (\sqrt{\frac{1-c_s^2}{f_0}}\sqrt{(A+4^{-(1+\lambda)(1+\mu)}(\lambda\phi^4)^{(1+\lambda)(1+\mu)})^{\frac{1}{1+\lambda}}})^{-1}\right)^{\frac{3}{2}} \end{aligned}$$

$$
\begin{aligned}
\times & \quad \left(\phi^4 \times \left(-1 + \frac{c_s M_p \lambda \phi}{\sqrt{\frac{3-3c_s^2}{f_0}} \sqrt{\left(A + 4^{-(1+\lambda)(1+\mu)} (\lambda\phi^4)^{(1+\lambda)(1+\mu)}\right)^{\frac{1}{1+\lambda}}}}^{\frac{1}{4}} \right) \right. \\
\times & \quad \left. (1-c_s^2)(c_s f_0 \alpha)^{-1}\right)^{\frac{1}{4}} \times \left(3\sqrt{\frac{1-c_s^2}{f_0}} M_p^4 \pi^{\frac{3}{2}} (1+\mu)^2 \phi \right)^{-1}. \qquad (3.3.6)
\end{aligned}
$$

$$
\begin{aligned}
N &= \sqrt{(A + 2^{-(1+\lambda)(1+\mu)} (\lambda\phi^4)^{(1+\lambda)(1+\mu)})^{\frac{1}{1+\lambda}}} (1 + \frac{2^{-(\lambda)(1+\mu)} (\lambda\phi^4)^{(1+\lambda)(1+\mu)}}{A} \\
&+ \quad 1)^{-} \frac{1}{2(1+\lambda)} Hypergeometric2F1 \times [-\frac{1}{4(1+\lambda)(1+\mu)}, -\frac{1}{2(1+\lambda)}, \\
&\times \quad 1 - \frac{1}{4(1+\lambda)(1+\mu)}, -\frac{2^{-(\lambda)(1+\mu)} (\lambda\phi^4)^{(1+\lambda)(1+\mu)}}{A}] \times (\sqrt{\frac{3-3c_s^2}{f_0}} \\
&\times \quad M_p \phi)^{-1}. \qquad (3.3.7)
\end{aligned}
$$

$$
\begin{aligned}
n_s &= 1 - \left(3(-1+c_s^2) M_p \sqrt{(A + V^{(1+\lambda)(1+\mu)})^{\frac{1}{1+\lambda}}} \phi \left((\lambda\phi^4)^{(1+\lambda)(1+\mu)} \right. \right. \\
&\times \quad \left(-6\sqrt{\frac{3-3c_s^2}{f_0}} \times \sqrt{(A + V^{(1+\lambda)(1+\mu)})^{\frac{1}{1+\lambda}}} + 7c_s M_p \lambda \phi + 16\mu \right. \\
&\times \quad \left. \left. \left(\sqrt{\frac{3-3c_s^2}{f_0}} \sqrt{(A + V^{(1+\lambda)(1+\mu)})^{\frac{1}{1+\lambda}}} c_s M_p \lambda \phi \right) \right) + 2^{2(1+\lambda)(1+\mu)} \\
&\times \quad A \left(2\sqrt{\frac{3-3c_s^2}{f_0}} \sqrt{(A + V^{(1+\lambda)(1+\mu)})^{\frac{1}{1+\lambda}}} (5+16\mu) - 32 c_s M_p \lambda^2 \right. \\
&\times \quad (1+\mu)\phi + \left(32\sqrt{\frac{3-3c_s^2}{f_0}} \sqrt{(A + V^{(1+\lambda)(1+\mu)})^{\frac{1}{1+\lambda}}} + 32\sqrt{\frac{3-3c_s^2}{f_0}} \right. \\
&\times \quad \left. \left. \left. \left. \sqrt{(A + V^{(1+\lambda)(1+\mu)})^{\frac{1}{1+\lambda}}} \mu - 9c_s M_p \phi - 32 c_s M_p \mu \phi \right) \right) \right) \right) \left(4 \left((A \right. \right. \\
&+ \quad V^{(1+\lambda)(1+\mu)})^{\frac{1}{1+\lambda}} 3(-1+c_s^2) + c_s \sqrt{\frac{3-3c_s^2}{f_0}} \sqrt{(A + V^{(1+\lambda)(1+\mu)})^{\frac{1}{1+\lambda}}} \\
&\times \quad \left. \lambda \phi f_0 M_p \right) \sqrt{\left(A + 2^{-2(1+\lambda)(1+\mu)} (\lambda\phi^4)^{(1+\lambda)(1+\mu)} \right)^{\frac{1}{1+\lambda}}} \Bigg)^{-1} \\
&\times \quad \left(4^{1+\lambda+\mu+\lambda\mu} A (\lambda\phi^4)^{(1+\lambda)(1+\mu)} \right). \qquad (3.3.8)
\end{aligned}
$$

$$
\begin{aligned}
\alpha &= \Bigg(3(-1+c_s^2)\sqrt{\frac{3-3c_s^2}{f_0}}M_p^2\phi^2(\lambda\phi^4)^{2(1+\lambda)(1+\mu)}\Bigg(-6\sqrt{\frac{3-3c_s^2}{f_0}}(A \\
&+ V^{(1+\lambda)(1+\mu)})^{\frac{2}{1+\lambda}}(1+2\mu)\times(-3+8\mu)+((A+V^{(1+\lambda)(1+\mu)})^{\frac{1}{1+\lambda}})^{\frac{3}{2}} \\
&\times 6c_sM_p\lambda(-6+\mu(3+32\mu))\phi-6c_s^3M_p((A+V^{(1+\lambda)(1+\mu)})^{\frac{1}{1+\lambda}})^{\frac{3}{2}} \\
&\times \lambda(-6+\mu(3+32\mu))\phi-c_s^2\sqrt{\frac{3-3c_s^2}{f_0}}(A+V^{(1+\lambda)(1+\mu)})^{\frac{1}{1+\lambda}}(1+2\mu) \\
&\times \Bigg(-6(A+V^{(1+\lambda)(1+\mu)})^{\frac{1}{1+\lambda}}(-3+8\mu)+f_0M_p^2\lambda^2(-7+16\mu)\phi^2\Bigg)\Bigg) \\
&+ 2^{4(1+\lambda)(1+\mu)}A^2\Bigg(6\sqrt{\frac{3-3c_s^2}{f_0}}(A+V^{(1+\lambda)(1+\mu)})^{\frac{2}{1+\lambda}}(5+16\lambda+16 \\
&\times (1+\lambda)\mu)-6c_sM_p((A+V^{(1+\lambda)(1+\mu)})^{\frac{1}{1+\lambda}})^{\frac{3}{2}}\lambda(9+32\lambda+32(1+\lambda)\mu) \\
&\times \phi+6c_s^3M_p((A+V^{(1+\lambda)(1+\mu)})^{\frac{1}{1+\lambda}})^{\frac{3}{2}}\lambda(9+32\lambda+32(1+\lambda)\mu)\phi \\
&+ c_s^2\sqrt{\frac{3-3c_s^2}{f_0}}(A+V^{(1+\lambda)(1+\mu)})^{\frac{1}{1+\lambda}}\Bigg(-6(A+V^{(1+\lambda)(1+\mu)})^{\frac{1}{1+\lambda}} \\
&\times (5+16\lambda+16(1+\lambda)\mu)+f_0M_p^2\lambda^2(9+32\lambda+32(1+\lambda)\mu)\phi^2\Bigg)\Bigg) \\
&\times 2^{3+2(\lambda+\mu+\lambda\mu)}A(\lambda\phi^4)^{(1+\lambda)(1+\mu)}\Bigg(-6\sqrt{\frac{3-3c_s^2}{f_0}}(A+V^{(1+\lambda)(1+\mu)})^{\frac{2}{1+\lambda}} \\
&\times \Bigg(20+32\lambda^2(1+\mu)^2+8\lambda(1+\mu)(7+8\mu)+\mu(41+32\mu)\Bigg)3c_sM_p \\
&\times ((A+V^{(1+\lambda)(1+\mu)})^{\frac{1}{1+\lambda}})^{\frac{3}{2}}\lambda\Bigg(81+163\mu+32(4\mu^2+4\lambda^2(1+\mu)^2 \\
&+ \lambda(1+\mu)(7+8\mu))\Bigg)\phi+3c_s^3M_p((A+V^{(1+\lambda)(1+\mu)})^{\frac{1}{1+\lambda}})^{\frac{3}{2}}\lambda\times\Bigg(81 \\
&+ 163\mu+32(4\mu^2+4\lambda^2(1+\mu)^2+\lambda(1+\mu)(7+8\mu))\Bigg)\times\phi+c_s^2 \\
&\times \sqrt{\frac{3-3c_s^2}{f_0}}(A+V^{(1+\lambda)(1+\mu)})^{\frac{1}{1+\lambda}}\Bigg(-6(A+V^{(1+\lambda)(1+\mu)})^{\frac{1}{1+\lambda}}\times\Bigg(20 \\
&+ 32\lambda^2(1+\mu)^2+8\lambda(1+\mu)(7+8\mu)+\mu(41+32)\Bigg)+f_0M_p^2\lambda^2 \\
&\times \Bigg(40+64\lambda^2(1+\mu)^2+16\lambda(1+\mu)(7+8\mu)+\mu(81+64\mu)\Bigg)\phi^2\Bigg)\Bigg)\Bigg) \\
&\times \Bigg(4\Bigg(3(-1+c_s^2)(A+V^{(1+\lambda)(1+\mu)})^{\frac{1}{1+\lambda}}+\sqrt{(A+V^{(1+\lambda)(1+\mu)})^{\frac{1}{1+\lambda}}}
\end{aligned}
$$

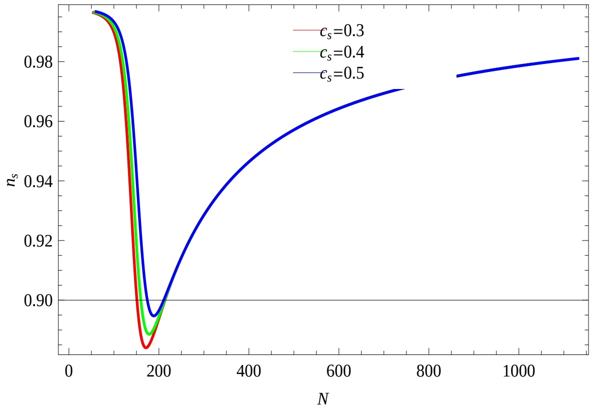

Figure 3.10: Plot of n_s versus N for different values of c_s. We have use the values of constant are $c_s = 0.3$, $c_s = 0.4$, $c_s = 0.5$, $M_p = 1$, $\lambda = 1$, $A = 1.5$, $f_0 = 93095.1$, $\alpha = 0.5$ and $\mu = 0.7$. We can find the best range of n_s where $60 < N$.

$$\times \quad \lambda\phi c_s\sqrt{\frac{3-3c_s^2}{f_0}}f_0M_p\Bigg)\sqrt{\left(A+2^{-2(1+\lambda)(1+\mu)}(\lambda\phi^4)^{(1+\lambda)(1+\mu)}\right)^{\frac{1}{1+\lambda}}}\Bigg)^{-1}$$
$$\times \quad \left(4^{1+\lambda+\mu+\lambda\mu}A(\lambda\phi^4)^{(1+\lambda)(1+\mu)}\right). \tag{3.3.9}$$

$$\begin{aligned} r \;=\; & 2^{\frac{9}{2}-4(\lambda+\mu+\lambda\mu)}c_sM_p\lambda^2(1+\mu^2)^2\phi^6(\lambda\phi^4)^{2(\lambda+\mu+\lambda\mu)}(A+4^{(-1-\lambda)(1+\mu)} \\ \times\; & (\lambda\phi^4)^{(1+\lambda)(1+\mu)})^{-2+\frac{2}{1+\lambda}}(\sqrt{\pi}((A+V^{(1+\lambda)(1+\mu)})^{\frac{1}{1+\lambda}})^{\frac{3}{2}}\gamma\Bigg(c_sM_p\lambda\phi \\ \times\; & \left(\sqrt{\frac{3-3c_s^2}{f_0}}\sqrt{(A+V^{(1+\lambda)(1+\mu)})^{\frac{1}{1+\lambda}}}\right)^{-1}\Bigg)^{\frac{5}{2}}\Bigg((1-c_s^2)\phi^4 \\ \times\; & \left(-1+\frac{c_sM_p\lambda\phi}{\sqrt{\frac{3-3c_s^2}{f_0}}\sqrt{(A+V^{(1+\lambda)(1+\mu)})^{\frac{1}{1+\lambda}}}}\right)(c_sf_0\alpha)^{-1}\Bigg)^{\frac{1}{4}}. \end{aligned} \tag{3.3.10}$$

We have plotted the graph of $n_s - N$ which is shown in Figure **3.10** using quartic potential. The intervals $[0.895, 0.9875]$, $[0.8955, 0.9875]$, $[0.8975, 0.9875]$ for red, green and blue lines shows the behavior of our graphs which is compatible with constraints of Planck TT,TE,EE+lowP+lensing data 2018 [105]. Figure **3.11** indicates the behavior of α versus N for quartic potential

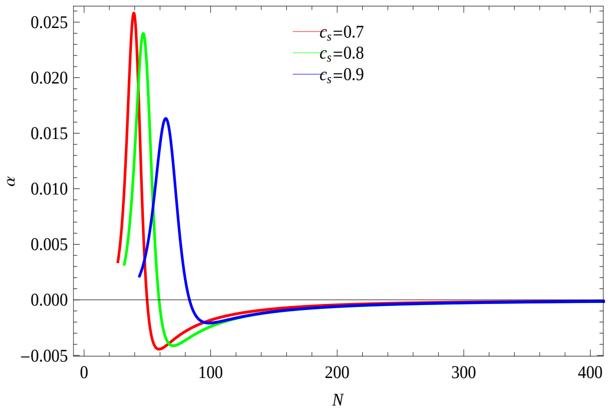

Figure 3.11: Plot of α versus N for different values of c_s. The constants parameters are $c_s = 0.7$, $c_s = 0.8$, $c_s = 0.9$, $M_p = 1$, $\lambda = 1$, $A = 4$, $f_0 = 3095.1$, $\alpha = 0.5$ and $\mu = 0.5$. We can find the best range of α where $60 < N$.

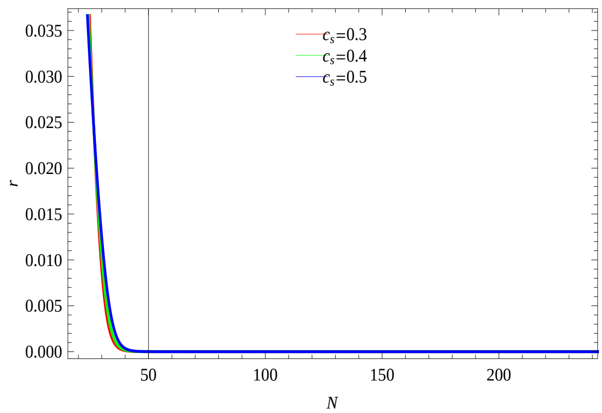

Figure 3.12: Plot of r versus N for different values of c_s in strong epoch. The constants parameters are $c_s = 0.3$, $c_s = 0.4$, $c_s = 0.5$, $M_p = 1$, $\lambda = 1$, $A = 4$, $f_0 = 3095.1$, $\alpha = 0.5$ and $\mu = 0.5$. We can find the best range of r where $60 < N$.

in the warm DBI scenario. The intervals $[-0.005, 0.025625]$, $[-0.004375, 0.02375]$, $[0.004725, 0.015625]$ for red, green and blue lines shows the behavior of our graphs which is compatible with constraints of Planck TT,TE,EE+lowP+lensing data 2018 [105]. The values of constants parameters are same as we use in Figure **3.11** leads to $r - N$ plane for quartic potential in the current set up of inflationary model. The intervals $[0, 0.036875]$, $[0, 0.036875]$, $[0, 0.036875]$ for red, green and blue lines shows the behavior of our graphs which is compatible with constraints of the Planck TT,TE,EE+lowP+lensing data 2018 [105].

Chapter 4
Summary

In this thesis, we have discussed the different Chaplygin gas models GCG and MCG in inflationary universe for FRW geometry by considering non-canonical scalar field model in the presence of specific form of AdS warp factor and potential (quartic and chaotic scalar field). We have modified the first Friedmann equation under slow-roll approximation to study the Chaplygin gas. Also, we have found the inflationary parameters which is constrained by Planck TT,TE,EE+lowP+lensing data (2018) [105]. We have studied the behavior of these inflationary parameters through planes such as $n_s - N$, $r - N$ and $\alpha - N$.

GCG Model for chaotic potential:

• In GCG model using chaotic potential for $c_s = 0.3, 0.4, 0.5$, in Figure (**3.1**) n_s lies in the range $0.972^{+0.02}_{-0.02}$ for the desired e-folds number and it is comparable with Planck TT,TE,EE+lowP+lensing data 2018 range which is 0.9649 ± 0.0042 [105].

• Figure (**3.2**) represents that α range lies in the range $-0.0005^{+0.001}_{-0.001}$ for observable e-folds number. This range is well matched with the range of observational Planck TT,TE,EE+lowP+lensing data 2018 [105].

• In Figure (**3.3**) the observed range of r in the current set up is $0.0004^{+0.0004}_{-0.0004}$ with respect to observable e-folds number. This range is comparable with the Planck data TT,TE,EE+lowP+lensing 2018 [105] range.

MCG Model for chaotic potential:

• In MCG model using chaotic potential for $c_s = 0.3, 0.4, 0.5$, in Figure (**3.4**) n_s lies in the range $0.97^{+0.02}_{-0.02}$ for the desired N of and it is comparable with the Planck TT,TE,EE+lowP+lensing data 2018 [105].

• Figure (**3.5**) represents that α range lies in the range $0.0015^{+0.0025}_{-0.0025}$ for observable N. This range is comparable with the range of observational

Planck TT,TE,EE+lowP+lensing data 2018 [105].

• In Figure (**3.6**) the observed range of r in the current set up is $0.125^{+0.125}_{-0.125}$ with respect to observable N. This range is comparable with the Planck data TT,TE,EE+lowP+lensing 2018 [105] range.

GCG Model for quartic potential:

• Using quartic potential in GCG model for $c_s = 0.3, 0.4, 0.5$, in Figure **3.7** our n_s lies in the range $0.97^{+0.05}_{-0.05}$ for the desired N and it is compatible with the Planck TT,TE,EE+lowP+lensing data 2018 range which is 0.9649 $\pm$0.0042 [105].

• For $c_s = 0.3, 0.4, 0.5$, this Figure **3.8** represents that α range lies in the range $0.0045^{+0.0055}_{-0.0055}$ for observable e-folds number. This range is compatible with range of observational Planck TT,TE,EE+lowP+lensing data 2018 that is 0.005 ± 0.013 [105].

• In Figure **3.9** the observed range of tensor-to-scalar in the current set up is $0.0045^{+0.0045}_{-0.0045}$ w.r.t observable N. This range is comparable with the Planck TT,TE,EE+lowP+lensing data 2018 range which is $r_{0.002} < 0.101$ [105].

MCG Model for quartic potential:

• Considering quartic potential in GCG model for $c_s = 0.3, 0.4, 0.5$ respectively, in Figure **3.10** the range of n_s $0.94^{+0.05}_{-0.05}$ for the desired N and it is comparable with the Planck data TT,TE,EE+lowP+lensing 2018 [105] range which is 0.9649 $\pm$0.0042.

• Figure **3.11** shows that α range lies in the range $0.01^{+0.015}_{-0.015}$ for observable N. This range is comparable with the range of observational Planck TT,TE,EE+lowP+lensing data 2018 [105] that is 0.005 ± 0.013.

• The observed range of r in Figure **3.12** is $0.0185^{+0.0185}_{-0.0185}$ w.r.t observable

N. This range is compatible with the Planck TT,TE,EE+lowP+lensing data 2018 [105] range which is $r_{0.002} < 0.101$.

Table 1: Combinations of Planck power spectra, Planck lensing and BAO.

$Parameter$	TT+lowE	TT,TE,EE+lowE	TT,TE,EE+lowE+lensing
n_s	0.9626 ± 0.0057	0.9649 ± 0.0044	0.9649 ± 0.0042
r	< 0.102	< 0.107	< 0.101
α	-0.004 ± 0.015	-0.006 ± 0.013	-0.005 ± 0.013

Chapter 5
References

[1] T. Ma and S. Wang, J. Math. Study, V **47**, 305-378 (2014).

[2] P. J. E. Peebles and Bharat Ratra, Rev. Mod. Phys. **75**, 559 (2013).

[3] B. Ratra and P. J. E. Peebles, Phys. Rev. D **37**, 3406(1988).

[4] A. Kamenshchik, U. Moschella and V. Pasquier, Phys. Lett. B **511**, 265-268 (2001).

[5] M. Li, Phys. Lett. B **603**, 1 (2004).

[6] A. Dev, J. S. Alcaniz and D. Jain, Phys. Rev D. **67**, 023515 (2003).

[7] P. Rudra, Mod. Phys. Lett. A **28**(2013)1350102.

[8] R. Herrera, M. Olivares, N. Videla, Eur. Phys. J. C **73**, 2295 (2013).

[9] A. H. Guth and S.-Y. Pi, Phys. Rev. Lett. **49**, 1110 (1982).

[10] A. D. Linde, Phys. Lett. B **108**, 389 (1982).

[11] A. Albrecht and P. J. Steinhardt, Phys. Rev. Lett. **48**, 1220 (1982).

[12] A. D. Linde, Phys. Lett. B **129**, 177 (1983).

[13] A. D. Linde, Lect. Notes Phys. **738**, 1 (2008).

[14] J. Martin, Braz. J. Phys. **34**, 1307 (2004).

[15] J. Martin, Lect. Notes Phys. **669**, 199 (2005).

[16] J. Martin, Lect. Notes Phys. **738**, 193 (2008).

[17] A. Starobinsky, Phys. Lett. B **91**, 99 (1980).

[18] A. Berera, Phys. Rev. Lett. **75**, 3218 (1995).

[19] A. Berera, Nucl. Phys. B **585**, 666 (2000).

[20] P. W. Higgs, Phys. Rev. Lett. **13**, 508 (1964).

[21] A. Pich, arXiv:0705.4264.

[22] K. Olive, Chinese Phys. C **40**, 100001 (2016).

[23] M. R. Setare, and V. Kamali,arXiv: 1508.05479[gr-qc].

[24] P. Franche, R. Gwyn, B. Underwood, and A. Wissanji, Phys. Rev. D **81**, 123526 (2010).

[25] X. Chen, J. (2005), arXiv:hep-th/0501184.

[26] X. Chen, Phys. Rev. D **71**, 063506 (2005).

[27] E. Silverstein and D. Tong, Phys. Rev. D **70**, 103505 (2004).

[28] M. Alishahiha, E. Silverstein, and D. Tong, Phys. Rev. D **70**, 123505 (2004).

[29] C. Armendariz-Picon, T. Damour, and V. Mukhanov, Phys. Lett. B **458**, 209 (1999).

[30] J. Garriga and V. Mukhanov, Phys. Lett. B **458**, 219 (1999).

[31] V. Mukhanov and A. Vikman, J. Cosmol. Astropart. Phys. **02**, 004 (2006).

[32] F. Helmer and S. Winitzki, Phys. Rev. D **74**, 063528 (2006).

[33] V. Taveras and N. Yunes, Phys. Rev. D **78**, 064070 (2008).

[34] N. Bose and A. S. Majumdar, Phys. Rev. D **80**, 103508 (2009).

[35] N. Bose and A. S. Majumdar, Phys. Rev. D **79**, 103517 (2009).

[36] P. Franche, R. Gwyn, B. Underwood, and A. Wissanji, Phys. Rev. D **82**, 063528 (2010).

[37] N. C. Devi, A. Nautiyal, and A. A. Sen, Phys. Rev. D **84**, 103504 (2011).

[38] S. Unnikrishnan, V. Sahni, and A. Toporensky, J. Cosmol. Astropart. Phys. **08**, 018 (2012).

[39] K. Rezazadeh, K. Karami, and P. Karimi, J. Cosmol. Astropart. Phys. **09**, 053 (2015).

[40] K. Rezazadeh, K. Karami, and S. Hashemi, Phys. Rev. D **95**, 103506 (2017).

[41] S. Alexander, R. H. Brandenberger, D. Easson, Phys. Rev. D **62**, 103509 (2000).

[42] P. J. Steinhardt, N. Turok, Phys. Rev. D **65**, 126003 (2002).

[43] J. Khoury, B. A. Ovrut, N. Seiberg, P. J. Steinhardt, N. Turok, Phys. Rev. D **65**, 086007 (2002).

[44] J. Khoury, B. A. Ovrut, P.J. Steinhardt, N. Turok, Phys. Rev. D **64**, 123522 (2001).

[45] J. Martin, P. Peter, N. Pinto Neto, D. J. Schwarz, Phys. Rev. D **65**, 123513 (2002).

[46] F. Finelli, R. Brandenberger, Phys. Rev. D **65**, 103522 (2002).

[47] R. Brandenberger, D. A. Easson, D. Kimberly, Nuclear Phys. B **623**, 421 (2002).

[48] R. Kallosh, L. Kofman, A. D. Linde, Phys. Rev. D **64**, 123523 (2001).

[49] J. Martin, P. Peter, N. Pinto-Neto, D. J. Schwarz, Phys. Rev. D **67**, 028301 (2003).

[50] P. Peter, N. Pinto-Neto, Phys. Rev. D **66**, 063509 (2002).

[51] S. Tsujikawa, R. Brandenberger, F. Finelli, Phys. Rev. D **66**, 083513 (2002).

[52] L. Kofman, A. D. Linde, V.F. Mukhanov, J. High Energy Phys. 0210 (2002).

[53] J. Martin, P. Peter, Phys. Rev. D **68**, 103517 (2003).

[54] J. Martin, P. Peter, Phys. Rev. D **69**, 107301 (2004).

[55] P. Peter, E.J. Pinho, N. Pinto-Neto, Phys. Rev. D **75**, 023516 (2007).

[56] F. Finelli, P. Peter, N. Pinto-Neto, Phys. Rev. D **77**, 103508 (2008).

[57] F. T. Falciano, M. Lilley, P. Peter, Phys. Rev. D **77**, 083513 (2008).

[58] L. R. Abramo, I. Yasuda, P. Peter, Phys. Rev. D **81**, 023511 (2010).

[59] R. Brandenberger, Phys. Rev. D **80**, 043516 (2009).

[60] R. H. Brandenberger, Classical Quantum Gravity, **28**, 204005(2011).

[61] Y.-F. Cai, D.A. Easson, R. Brandenberger, JCAP, **1208**, 020 (2012).

[62] C. Cheung, P. Creminelli, A. L. Fitzpatrick, J. Kaplan and L. Senatore, JHEP **0803**, 014 (2008).

[63] S. Weinberg, Phys. Rev. D **77**, 123541 (2008).

[64] D. Boyanovsky, Phys. Rev. D **92**, 023527 (2015).

[65] D. Boyanovsky, Phys. Rev. D **93**, 043501 (2016).

[66] J. Martin, C. Ringeval and V. Vennin, Phys. Dark Univ. **5-6**, 75 (2014).

[67] I. G. Moss, Phys.Lett.B 154, **120** (1985).

[68] A. Berera, Phys. Rev. D **55**, 3346 (1997).

[69] E. Hubble, Proc. N.A.S. **15**, 168 (1929).

[70] A. Friedmann, Z. Phys. **21**, 326 (1924).

[71] H. P. Robertson, Astrophys. J **82**, 284 (1935).

[72] A. G. Walker, Proc. London Math. Soc. 42, 90 (1937).

[73] G. Lemaitre, Gen. Rel. Grav. 29, 641 (1997).

[74] P. A. Ade, et al. Astronomy and Astrophysics **A1**, 571 (2014).

[75] A. R. Liddle, and D. H. Lyth, Cambridge, UK. Univ. Pr. 400 (2000).

[76] E. R. Harrison, Phys. Rev. D **1**, 2726 (1970).

[77] Y. B. Zeldovich, Astron. Astrophys. **5**, 84 (1970).

[78] B. A. Bassett, S. Tsujikawa, and D. Wands, Rev. Mod. Phys. **78**, 537 (2006).

[79] A. Berera and L.-Z. Fang, Phys. Rev. Lett. **74**, 1912 (1995).

[80] A. Berera, Phys. Rev. D **55**, 3346 (1997).

[81] A. Yu. Kamenshchik, U. Moschella and V. Pasquier, Phys. Lett. B 511, 265 (2001).

[82] H.-S- Tsien, J. Aeron. Sci. **6**, 339 (1939), T. von Karman, J. Aeron. Sci. ,**8** 337 (1941).

[83] Monerat, G.A. et al.: Phys. Rev. D 76, 02017 (2007), H. B. Benaoum, U. Debnath, A. Banerjee, and S. Chakraborty, Class. Quantum Grav. **21**, 5609 (2011).

[84] A. Linde, arXiv:0705.0164 [hep-th].

[85] F. L. Bezrukov, A. Magnin and M. Shaposhnikov, Phys. Lett. B **675**, 88 (2009); N. Okada, M. U. Rehman and Q. Shafi, Phys. Rev. D **82**, 043502 (2010).

[86] A. Berera and R. O. Ramos, Phys. Lett. B **607**, 1 (2005); A. Berera and R. O. Ramos, Phys. Rev. D **63**, 103509 (2001).

[87] S. Bartrum, M. Bastero-Gil, A. Berera, R. Cerezo, R. O. Ramos, and J. G. Rosa, Phys. Lett. B **732**, 116 (2014).

[88] H. Peiris, D. Baumann, B. Friedman, and A. Cooray, Phys. Rev. D **76**, 103517 (2007).

[89] M. Spalinski, Phys. Lett. B **650**, 313 (2007).

[90] D. Bessada, W. H. Kinney, and K. Tzirakis, J. Cosmol. Astropart. Phys. **09**, 031 (2009).

[91] A. G. Muslimov, Class. Quant. Gravity **7**, 231 (1990).

[92] D. S. Salopek and J. R. Bond, Phys. Rev. D **42**, 3936 (1990).

[93] W. H. Kinney, Phys. Rev. D **56**, 2002 (1997).

[94] M. Spalinski, J. Cosmol. Astropart. Phys. **04**, 018 (2007).

[95] Y.-F. Cai, J. B. Dent, and D. A. Easson, Phys. Rev. D **83**, 101301 (2011).

[96] A. R. Liddle and S. M. Leach, Phys. Rev. D **68**, 103503 (2003).

[97] S. Dodelson and L. Hui, Phys. Rev. Lett. **91**, 131301 (2003).

[98] H. Peiris, D. Baumann, B. Friedman, and A. Cooray, Phys. Rev. D **76**, 103517 (2007).

[99] D. Bessada, W. H. Kinney, and K. Tzirakis, J. Cosmol. Astropart. Phys. **09**, 031 (2009).

[100] M. Alishahiha, E. Silverstein, and D. Tong, Phys. Rev. D **70**, 123505 (2004).

[101] O. Aharony, S. S. Gubser, J. Maldacena, H. Ooguri, and Y. Oz, Phys. Rep. **323**, 183 (2000).

[102] Pich, A.: arXiv:0705.4264[hep-ph].

[103] L. H. Ford, Phys. Rev. D **35**, 2955 (1987).

[104] M. S. Bento, O. Bertolami, O. Sen, Phys. Rev. D **66**, 043507 (2002).

[105] N. Aghanim et al, arXiv:1807.06209 [astro-ph.CO](2018).